frontiers in Earth Science

ORIGINAL RESEARCH
published: 20 April 2021
doi: 10.3389/feart.2021.633820

Re-Evaluating the Surface Rupture and Slip Distribution of the AD 1609 M7 $^{1}/_{4}$ Hongyapu Earthquake Along the Northern Margin of the Qilian Shan, NW China: Implications for Thrust Fault Rupture Segmentation

Xiongnan Huang, Xiaoping Yang, Haibo Yang, Zongkai Hu and Ling Zhang*

State Key Laboratory of Earthquake Dynamics, Institute of Geology, China Earthquake Administration, Beijing, China

OPEN ACCESS

Edited by:
Maryline Le Béon,
National Central University, Taiwan

Reviewed by:
Yang Dao Yuan,
Lanzhou University, China
Austin Elliott,
United States Geological Survey, United States

***Correspondence:**
Xiongnan Huang
xiongnan_h@sohu.com

Specialty section:
This article was submitted to Structural Geology and Tectonics, a section of the journal Frontiers in Earth Science

Received: *26 November 2020*
Accepted: *05 February 2021*
Published: *20 April 2021*

Citation:
Huang X, Yang X, Yang H, Hu Z and Zhang L (2021) Re-Evaluating the Surface Rupture and Slip Distribution of the AD 1609 M7 $^{1}/_{4}$ Hongyapu Earthquake Along the Northern Margin of the Qilian Shan, NW China: Implications for Thrust Fault Rupture Segmentation. Front. Earth Sci. 9:633820. doi: 10.3389/feart.2021.633820

The Hexi Corridor is located beyond the northeastern edge of the Tibetan Plateau, and it is bounded by a series of active thrusts along the northern margin of the Qilian Shan and the southern piedmont of the Longshou Shan. Historically, five destructive earthquakes have occurred along the Hexi Corridor, which indicates that this region poses high potential seismic risks. The 1609 Hongyapu earthquake occurred along the Fodongmiao-Hongyazi fault in the northern Qilian Shan, China, and it killed more than 840 people and destroyed a large number of buildings. Presently, there are different opinions as to the distribution and length of the surface rupture of this event along the Fudongmiao–Hongyazi fault. Thus, we searched all of the fault scarps on the Holocene surfaces and suspected surface rupture locations related to the 1609 earthquake based on previous studies and developed detailed remote-sensing interpretations along the fault. An abundance of north-facing scarps on the younger fans and terrace faces, slightly higher than the active modern stream bed, were found along the Fodongmiao-Hongyazi fault in the area ranging from the Hongshuiba River (39.52°N, 98.41°E) in the west to the Shuiguan River (39.07°N, 99.37°E) in the east. Based on our research, we estimate a surface rupture length as ~98 km based on the distribution of the fault scarps on Late Holocene surfaces and constraints provided by age dating. Most of the surface ruptures are preserved as fault scarps and indicate an average vertical surface offset of ~1.0 m, a value found consistently in three segments of the fault. The surface rupture features indicate that segments of the fault ruptured together coseismically during the 1609 earthquake, i.e., a multisegment rupture. Using the surface fault traces, length of 98 or 90 km (without the Shuiguan River section), dip of 30° inferred from previous reflection profiles, a rigidity of 3.3×10^{10} N/m^2, and dip slip average as 1.9 m converted from our observations of the offsets, we computed the magnitude of this event as ca. Mw 7.2–Mw 7.4.

Keywords: fodongmiao-hongyazi fault, northern Qilian Shan, 1609 Hongyapu earthquake, surface rupture, thrust fault, rupture segmentation

INTRODUCTION

Mapping of the surface rupture features and geological effects of large earthquakes, as well as the distribution of slip, is useful for assessing regional seismotectonics (Yeats et al., 1996; Molnar and Ghose, 2000; Arrowsmith et al., 2016). However, lack of an apparent surface rupture is a common finding on low angle thrust faults associated with major historical earthquakes, and the reason could be related to little or no slip in the shallow part of the fault during such events (Kumar et al., 2006; Wang and Fialko, 2015). Alternatively, the reason could be related to the topographic features of the thrust earthquake surface ruptures. Thrusts tend to produce discontinuous and broad scarps, which are often ambiguous and less well preserved than normal or strike-slip fault breaks (Wells and Coppersmith, 1994; McCalpin, 2009; Arrowsmith et al., 2016). Importantly, floods may destroy coseismic surface scarps and stratigraphic records in just a few seasons (Sapkota et al., 2013). However, recent studies were able to locate the surface rupture of the AD 1934 Mw 8.2 Bihar–Nepal earthquake and 1950 Mw ~8.6 Assam earthquake by geomorphological mapping and age dating, which had previously been ascribed to blind faults (Sapkota et al., 2013; Priyanka et al., 2017).

Earthquake size is controlled primarily by the area of the fault plane that ruptures, as well as the amount of displacement averaged over this area (Scholz, 2002). Disjointed segments of faults can behave as distinct faults, rupturing separately in individual earthquakes, but at times these segments coalesce and rupture simultaneously in a large, entire-fault encompassing event (Sieh, 1996; Elliott et al., 2009). Thrust rupture segment boundaries may be indicated by different kinds of structural discontinuities along the fault, such as a strike-slip tear fault, sharp changes in the orientation of the fault, abrupt changes in dip, and so forth (Davis et al., 2005; Yue et al., 2005; McCalpin, 2009; Dal Zilio et al., 2020; Lei et al., 2020).

The Hexi Corridor in Gansu Province, China, was part of the Silk Road that formed during the Han Dynasty. It spans the transpressional region between the Altyn Tagh fault and Haiyuan fault, two regional left-lateral strike-slip faults at the northeastern corner of the Tibetan Plateau, and it is bounded mainly by a series of active thrusts along the northern piedmont of the Qilian Shan and the southern piedmont of the Longshou Shan (Xu et al., 2010) (**Figure 1**). The Hexi Corridor is located in arid or semi-arid areas, and surface ruptures of many historical earthquakes have been preserved here (Zheng, 2009a; Xu et al., 2010; Guo et al., 2019). Historically, five destructive earthquakes occurred along the Hexi Corridor, including the AD 180 $M7^1/_2$ Gaotai earthquake, AD 1609 $M7^1/_4$ Hongyapu earthquake, AD 1927 M8.0 Gulang earthquake, AD 1932 Mw 7.6 Changma earthquake, and AD 1954 M7.3 Shandan earthquake, which have been the focus of many previous studies (Gu, 1983; Lanzhou Institute of Seismology and State Seismological Bureau, 1985; Tapponnier et al., 1990; Lanzhou Institute of Seismology, 1992; Institute of Geology, State Seismological Bureau, and; Lanzhou Institute of Seismology, 1992; Chen, 1994; Earthquake Disaster Prevention Department and State Seismological Bureau, 1995; Gaudemer et al., 1995; Zheng et al., 2009b; Cao, 2010; Xu et al., 2010; Guo et al., 2019).

There is an agreement that the 1609 Hongyapu earthquake occurred along the Fudongmiao–Hongyazi fault (FHF), but the distribution and length of the 1609 surface rupture are still in dispute, as only a few detailed field observations have been published (Institute of Geology, State Seismological Bureau, and Lanzhou Institute of Seismology, 1992; Cao et al., 2010; Xu et al., 2010; Liu et al., 2012; Liu et al., 2014; Huang et al., 2018a). Notably, the distribution and magnitude of the slip along the rupture have not been clearly reported before our work (Huang et al., 2018a).

Field documentation of the preserved 1609 earthquake rupture was the focus of this study. We provide descriptions of the surface rupture based on field investigations, with more details compared to our previous report (Huang et al., 2018a). The offsets along the rupture were systematically reviewed, and the surface rupture slips were calculated according to rupture fault dip angles. Based on the surface slip distribution and the previous paleo-seismic trenching works (Huang et al., 2018b), the rupture segmentation of the FHF was discussed and the data were suggestive of a multisegment rupture for the 1609 earthquake. Our description of the fault trace, the length, and the slip distribution, and our estimate of the geological moment contributes to the limited dataset on large reverse-faulting earthquakes.

GEOLOGICAL SETTING AND OVERVIEW OF THE AD 1609 EARTHQUAKE

The Qilian Shan is the youngest uplifting orogenic belt in NE Tibet (**Figure 1**) (Meyer et al., 1998; Tapponnier et al., 2001; Hetzel et al., 2002; Zhang et al., 2004). The late Cenozoic deformation of this range recorded the remote effects of the Indo-Asian collision (Tapponnier et al., 2001; Zhang et al., 2004; Yuan et al., 2013), and the present crustal shortening rate maintains a high level of 5. 5–7 mm/a as shown by geodetic measurements (Zhang et al., 2004; Zheng et al., 2013). The northern Qilian thrust fault zone, which is located on the northern margin of the Qilian Shan, has accumulated approximately 20% of the crustal shortening of the Qilian block (Tapponnier et al., 1990; Hetzel et al., 2004; Zheng et al., 2013; Zuza et al., 2016; Yang et al., 2018a; Yang et al., 2018b; Hetzel et al., 2019). High fault slip rates and the historic occurrence of strong earthquakes indicate that there are high potential seismic risks within this fault zone (Hetzel et al., 2004; Xu et al., 2010; Hetzel et al., 2019).

The Fodongmiao-Hongyazi fault (FHF) is a major range-bounding thrust fault between the Qilian Shan and Jiudong basin, belonging to the middle segment of the northern Qilian thrust fault zone (**Figures 1**, **2**) (Yang et al., 2018a). The segment of the FHF that has been the most active during the Late Quaternary is approximately 110 km long, and it trends WNW (Institute of Geology, State Seismological Bureau, and Lanzhou Institute of Seismology, 1992; Chen, 2003; Zheng et al., 2009b; Xu et al., 2010; Liu et al., 2011; Liu et al., 2012; Liu et al.,

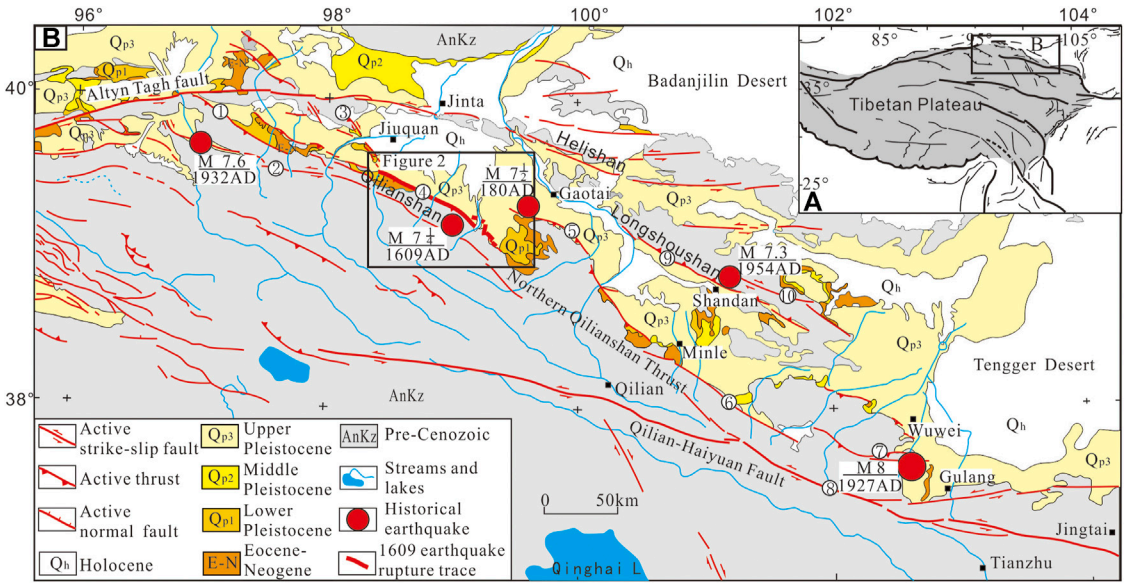

FIGURE 1 | (A) Active tectonics map of northeastern Tibet (after Xu et al., 2010). Fault labels in **(B)** include: 1) Hanxia–Dahuanggou thrust; 2) Changma fault; 3) Jiayuguan thrust; 4) Fudongmiao–Hongyazi thrust; 5) Yumushan thrust; 6) Minle–Damayin thrust; 7) Dongqingding thrust; 8) Lenglonglin; 9) south Longshoushan thrust; 10) Baode fault.

2014; Yang et al., 2017; Yang et al., 2018a, Yang et al., 2018b; Liu et al., 2019). The vertical slip rate of the FHF has amounted to 1.2 ± 0.1 m/ka during the last 200 ka (Hetzel et al., 2019).

This fault can be subdivided into three segments by the Hongshan village and Maying River based on the fault trace geometry and local structures (Yang et al., 2017). We adopted this segmentation in this study.

The western segment of the FHF has a relatively continuous fault trace along the piedmont foreland with a strike of 115°, and there are uplifted and dissected fans in the hanging wall. The surface fault dips south with a dip angle of 25–45° as measured on the outcroppings in trenches, gullies, and river banks. The seismic reflection profile across the Ciyaokou village revealed a south fault dip of 30° in depth (Yang et al., 2007). The hanging wall is mainly Neogene mudstone and sandstone, and a few Oligocene and Early Cretaceous rocks are present.

The middle segment has a sinuous and discontinuous trace along the mountain front, with a strike of 120°. The highest peak of the Qilian Shan at an elevation of 5,564 m is located on this segment. The outcrops of the hanging wall are mainly Paleozoic granite and the foot wall are mainly Quaternary alluvium. The fault dips south with a surface dip angle of approximately 40° according to field observations (Yang et al., 2017; Yang et al., 2018a; Yang et al., 2018b), but the value can range from 25° to 35° at depth based on seismic reflection profiles (Zuza et al., 2016).

The eastern segment is separated from the middle section by the Hujiatai anticline in the Maying River area. The surface trace occurs along the piedmont fans or the mountain front, and it includes fault scarps and fold-scarps; the overall trend is approximately 130°. The hanging wall is mainly Paleozoic sandstone and mudstone, and a few Mesozoic and Tertiary rocks are outcropped in the Maying River area. The fault dips south with a dip angle of 20–70° at the surface according to measurements taken in the field (Yang et al., 2017; Yang et al., 2018a; Yang et al., 2018b), and the dip is 25–30° at depth based on seismic reflection profiles (Yang et al., 2007; Zuza et al., 2016).

The 1609 Hongyapu earthquake killed more than 840 people and destroyed a large number of buildings, including those in the old town of Hongyapu (Li, 1960; Gu, 1983; Lanzhou Institute of Seismology and State Seismological Bureau, 1985; State Seismological Bureau, and Lanzhou Institute of Seismology, 1992; Institute of Geology, 1993; Cao, 2010; Liu et al., 2011). Scarps, cracks, caves, and landslides caused by the earthquake were observed by scientific research teams in the Hongyazi village and its surrounding area in the 1960s (Cao, 2010). Differing views on the epicenter location and magnitude of this earthquake exist among different research groups, based on their estimates on field work and textual analyses. Li (1960) suggested that the epicenter was in the area southeast of Jiuquan (39.2°N, 99.1°E), and the magnitude of the event was $6^1/_2$, based on the analysis of buildings damage and life loss from textual analyses. Gu (1983) and (Earthquake Disaster Prevention Department, 1995) State Seismological Bureau (1995) increased the magnitude to $7^1/_4$ and changed the epicenter to the area of 39.2°N, 99.0°E according to the macroseismic intensity distribution based on more detailed textual analyses and field observations of damages. Meanwhile, Lanzhou Institute of Seismology, State Seismological Bureau (1985) suggested that the magnitude of the event was $7^1/_4$ and the epicenter was in the area of Hongyapu (39.2°N, 99.2°E) with a different macroseismic intensity distribution map. The Institute of Geology, State Seismological Bureau, and Lanzhou Institute of Seismology (1992) adopted the same magnitude of $7^1/_4$ and the same seismic intensity map from Lanzhou Institute of Seismology,

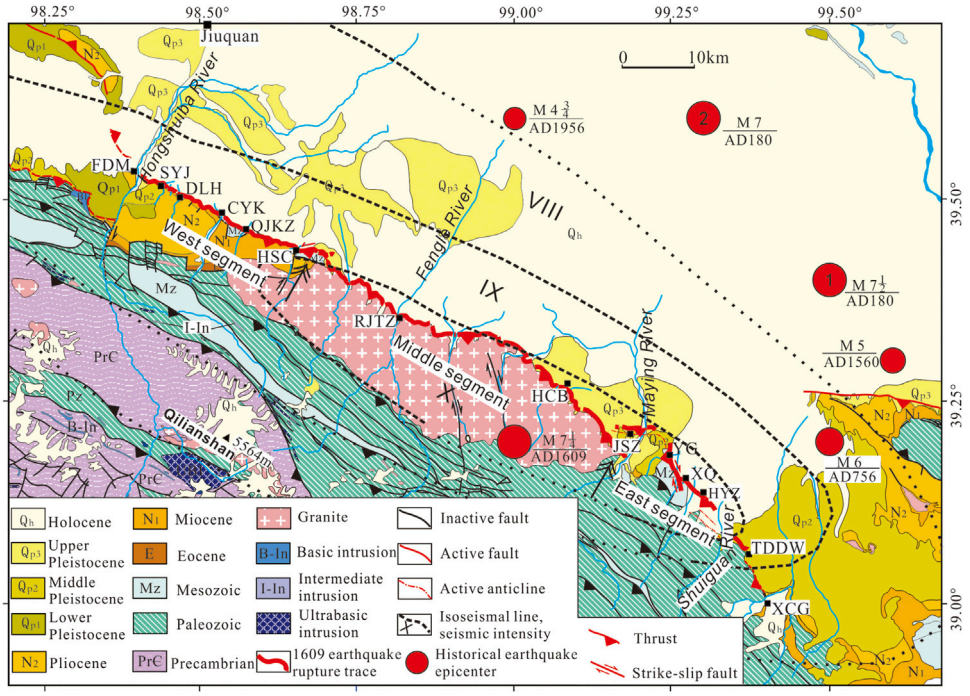

FIGURE 2 | Geologic map across the Fodongmiao-Hongyazi fault. Place names: FDM, Fodongmiao; SYJ, Shiyangjuan; DLH, Dalong River; CYK, Ciyaokou; QJKZ, Qujiakouzi; HSC, Hongshan Village; RJTZ, Rujiataizi; HCB, Huangcaoba; JSZ, Jiashazi Reservoir; YG, Yagou; XQ, Xiaoquan; HYZ, Hongyazi; TDDW, Toudaodongwan; XCG, Xichagou. The segmentation is according to Yang et al. (2017). The isoseismal lines of the 1609 earthquake are after Liu et al. (2011). Locations of historical earthquake epicenters, shown by red circles in the figure, are from the Earthquake Disaster Prevention Department and State Seismological Bureau (1995), Earthquake Disaster Prevention Department, China Earthquake Administration (1999), and Cao et al. (2010). The 180 AD M7.5 and 180 AD M7.0 data are for the same event but data vary in accordance with different estimates; these data are from the Earthquake Disaster Prevention Department and State Seismological Bureau (1995) and Cao et al. (2010), respectively.

State Seismological Bureau (1985), but proposed that the epicenter was in the west of Xiaoquan (39°0′54″N, 99°16′E) according to their field work on the earthquake surface ruptures. Liu et al. (2011) provided new evidences for the macroseismic intensity assessment of the earthquake to draw a new seismic intensity map and suggested that the meizoseismal intensity value reached X, the long axis was more than 70 km striking NWW (**Figure 2**), and the epicenter was in the area west of Hongyazi village (39.2°N, 99.0°E).

There are also different opinions on the distribution and length of the surface rupture at present. The Institute of Geology, State Seismological Bureau, and Lanzhou Institute of Seismology (1992) suggested that the length of the surface deformation zone is approximately 60 km long and consists of scarps, mole tracks, cracks, and an offset of streams and ridges from the Fengle River in the west to the Bailang River west bank in the east. Xu et al. (2010) proposed that the Hongyapu earthquake was accompanied by two segments of rupture, namely, the Xiaoquan segment that strikes N15°W with a coseismic rupture length of 11 km, and the Hongyazi segment that strikes N65°W with a coseismic rupture length of 5 km. Cao (2010) suggested that the surface rupture of the Hongyapu earthquake is approximately 90 km long with a maximum vertical offset of 2 m and lateral offset of 3 m, and it occurs as fault scarps and a few left-lateral offset rills locally. Liu et al. (2012), Liu et al. (2014) reported that the coseismic rupture of the Hongyapu earthquake occurs as small fault scarps with fresh free faces along the middle and western section of the FHF. Importantly, previous research only reported limited coseismic displacement data for this earthquake and did not systematically document the distribution and magnitude of slip along the rupture.

Furthermore, there were insufficient constraints from age dating on the surface rupture before our work. The Institute of Geology, State Seismological Bureau, and Lanzhou Institute of Seismology (1992) reported two thermoluminescence ages in the gully profile near the Xiaoquan village. Additionally, Xu et al. (2010) provided some age dating results for the fan surfaces across the Xiaoquan fault to constrain the surface rupture in the Xiaoquan area, and they suggested that no coseismic rupture occurred in the area west of the Maying River during the 1609 earthquake based on thermoluminescence dating results of alluvial fans. The Group of Liu (Cao, 2010; Liu et al., 2012; Liu et al., 2014) reported a dozen optically stimulated luminescence measurements and several ^{14}C dating results for alluvial fans and the terrace surface across the FHF, but most of the data were older than 6 ka BP and only rare data points from were recovered for the Late Holocene.

During our mapping on the FHF at 1:50,000 from 2014 to 2017, we searched all of the small fault scarps on the Holocene

surfaces and the suspected surface rupture potentially related to the 1609 earthquake after reviewing previous studies on the FHF; then, we developed remote-sensing interpretations for the fault. In our field work, we found an abundance of north-facing scarps on the younger fans and terrace faces, which are slightly higher than the active yongest stream bed, along the FHF from the Hongshuiba River (39.52°N, 98.41°E) in the west to the Shuiguan River (39.07°N, 99.37°E) in the east, with a total length of approximately 98 km. Some of these scarps preserve the free face with heights of 0.2–0.9 m. Additionally, the profiles of gullies, riverbanks, and trenches across the scarps revealed that most of these were controlled by faults, as indicated by the south dip faults in the profile data under the scarps. Rills and stream terraces are right-lateral offset along the east-west strike scarps trace in the east of the Hongshan village and left-lateral offset along the north-south strike scarps trace in the west of the Xiaoquan village, compatible with a uniform overall North-east slip direction. In our field observations, we emphasized keys areas mapped for the rupture at a 1:50,000 scale on topographic and aerial photographic base maps, measurements of the surface offset, and detailed observations at numerous sites. We focused on the fault scarps on Late Holocene fans and terrace surfaces, as constrained by optically stimulated luminescence and ^{14}C dating, samples from the trenches and pits on the young and deformed surfaces.

METHODS AND DEFINITION OF TERMS

Methods

We first mapped the track of the FHF on the Google Earth imagery before the field work. Fault scarps were initially detected from inspection of Google Earth imagery, and targeted for detailed field survey. We performed 94 offset determinations using a combination of profile data obtained by a differential global positioning system (GPS), tape and compass, unmanned aerial vehicle (UAV) photography, and simple field measurements with a laser distance meter. We also recorded, the strike of the fault, and the dip where the exposure is available.

Differential GPS was used to measure the locations and elevations of points with 0.5 m spacing along a profile normal to the strike on the surface across the fault trace with a precision of 0.1 m. An unmanned aerial vehicle with a 4 K camera was used to scan the deformed area. Stereo images were used to generate a high-resolution DEM with Agisoft Photoscan. To ensure the accuracy of the DEM, 19 control points were set uniformly across the scanned area and precisely located with real-time kinematic GPS to 0.2 m vertical precision. The resulting DEMs was previously partially published by Yang et al. (2017) with elevation error of 0.05 m and location error of 0.05–0.1 m, and here we analyzed these data to determine surface offsets. A line profile normal to the strike is used to extract the surface offset across the fault trace. We also use tape and compass to determine surface offset. Along a line normal to the fault scarp, spacings of the neighbor points were measured by a tape with precision of 0.01 m and surface slope angles, dip, were measure by a compass with precision of 0.5° at every point. And then we plot the points with spacings and dips on a plane to get a line profile across the scarps. The method of Thompson et al. (2002) was applied to calculate the vertical displacement and errors of offset alluvial fans and terraces.

Portion of vertical offsets and total lateral offsets were surveyed by handheld laser range finder, with a vertical and horizontal precision of 0.3 m. We measured the altitude at the crest and toe of the scarp, and calculate the altitude difference to get the scarp height. As most of the horizontal distances are narrower than 2 m, so the scarp heights measured by handheld laser range finder are very close to the vertical offset. For the lateral offsets, we measured horizontal distances between the offset channel margins or the offset thalwegs, which intersect and are nearly perpendicular to the fault by laser range finder.

In our offset tabulation (**Supplementary Table S1**), we assigned a relative quality rating for the offsets from our confidence in the offset reconstruction and its applicability to the 1609 event. We calculated the most recent slips from the offsets with the rupture fault dip angle determined by trench work and field work on the fault exposures. The rupture trace, assumptions of dip and seismogenic thickness, and conversion to dip slip from our offset observations enabled us to estimate the moment contribution from the rupture.

Characteristics of Thrust Fault Scarps and Identification of the Most Recent Fault Slip

The surface rupture of the 1609 earthquake mainly exists as thrust fault scarps. These scarps can be divided into three types according to their different topographical characteristics and origins. We evaluated the measurements on the scarps in different ways to achieve accurate displacement estimates of this most recent earthquake (**Figure 3**). The types of scarps encountered are described below.

1) Simple fault scarp exists on different surfaces as a continuous single fault trace (**Figure 3A**). This type of scarp is suggested to have formed by a fault with only one branch, i.e., a breaching surface along the same track during different earthquake events. The most recent vertical slip of the fault can be acquired by measuring the surface offset across the lowest scarps on the young surface. We took the vertical offset of the surface as the vertical slip in this study, and the variance between these values is small because the majority of slope angles of the young surfaces are less than 5°. Additionally, we took the scarp height as an approximation of the vertical offset on lower scarps, as the scarp height is close to the vertical offset but slightly larger, and these data are marked as low-quality data in our database (**Supplementary Table S1**). Free faces have been found not only on lower scarps, but also on the higher composite fault scarps, and these are mainly composed of gravels with no or minimal loose cover (**Figure 3B**). The free faces on the thick-layered loose covered surface could have retreated and been eliminated over a short time, while boulders in the gravel layer protected the free face from erosion and

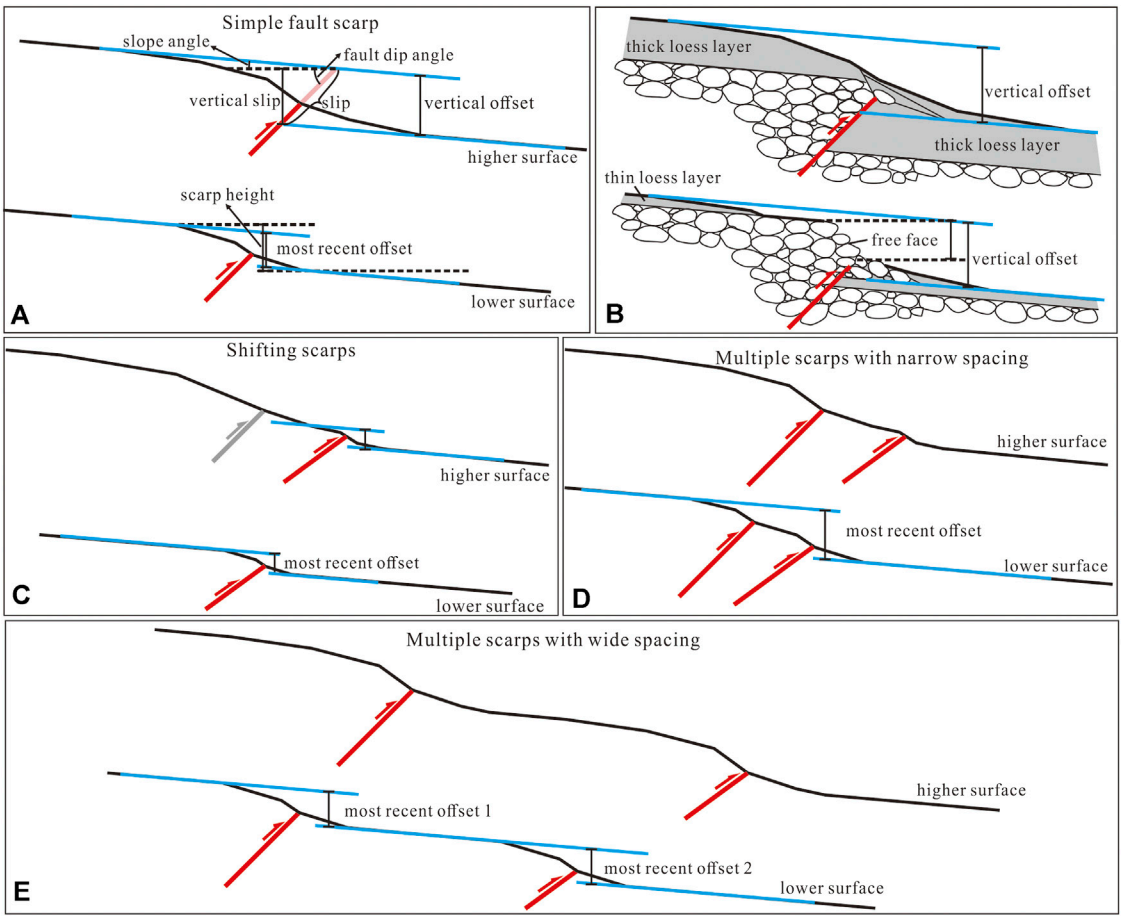

FIGURE 3 | Scarp types of the 1609 earthquake. **(A)** Simplified model for the simple fault scarp. The upper figure shows a higher and older scarp on an older and higher surface, and the lower one is a lower scarp on a young surface. The vertical slip is very close to the vertical offset of the surface according to the upper figure, and the scarp height is similar but slightly larger than the offset according to the lower figure. **(B)** The free face is prone to remain on the surface, which is mainly composed of gravels with minimal loose cover, and its height is approximate to the vertical offset. **(C)** Simplified model for shifting scarps. A steep and lower scarp occurs on the hillslope of an older modified scarp on the higher surface, while only one scarp occurs on the adjacent lower surface. **(D)** Multiple scarps with narrow spacing, less than a hundred meters, can be profiled on the young surface to achieve the most recent offset. **(E)** Multiple scarps with wide spacing, more than hundreds of meters. We summed up all offsets across each scarp on the young surface to obtain the total vertical offset of the most recent earthquake.

thus these were preserved much longer. We also used the height of the free face as an approach to estimating the vertical offset.

2) Shifting scarps often occur in this region as two parallel tracks of scarps with greatly different heights (**Figure 3C**). These always present as a small and steeper scarp on the hillslope of a large composite scarp. Their formation could have been driven by the propagation of the thrust fault zone, whereby the old splays of the fault zone stopped breaching while a new splay encroached into the adjacent region and the surface rupture locations shifted forward. There is only one scarp on the lower and younger surface beside the shifting scarps. The surface offset across the lower scarp of shifting scarps can be used to evaluate the vertical slip of the newest earthquake.
3) Multiple scarps occur here as several parallel scarps on the same surface (**Figures 3D,E**). In this type of scarp, the scarp on the newer surface is lower than the one on the older surface while tracing along the same track. The vertical displacement of the newest event can be assessed by measuring the total vertical offset of the young surface across the multiple scarps as the spacing between scarps is narrow (**Figure 3D**). If the spacing was too large, i.e., more than hundreds of meters, we measured every scarp separately and summed up the most recent offsets to obtain the total vertical displacement (**Figure 3E**).

RESULTS

Offset Landforms and the Most Recent Fault Slip at Different Sites

Hongshuiba River Site

On the right bank of the Hongshuiba River, five levels of fluvial terraces, namely, T5–T9 (we named the lowest terrace as T1, and

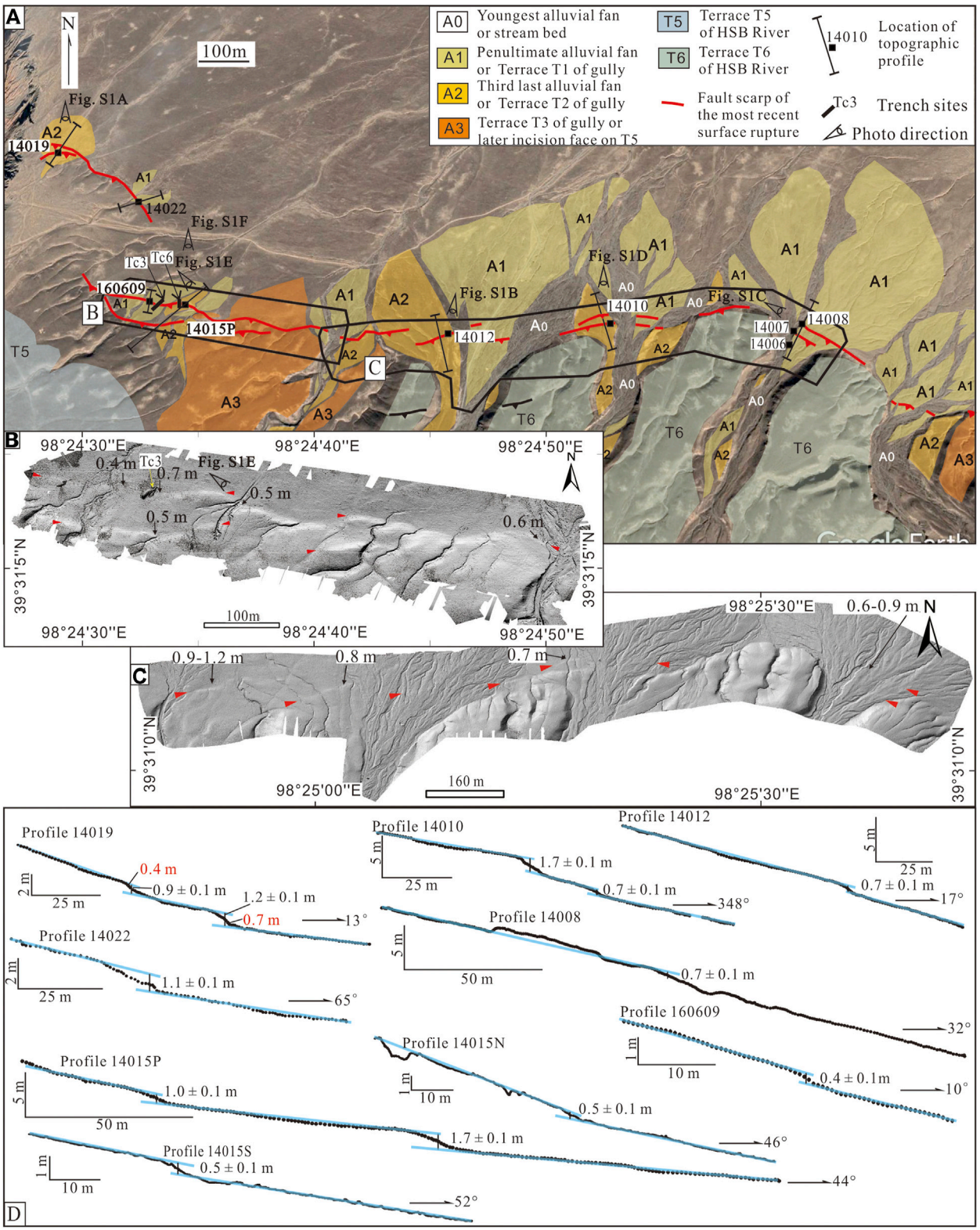

FIGURE 4 | Topographic features of the 1609 earthquake surface rupture on the Hongshuiba River site. **(A)** Surface rupture map. **(B,C)** Hillshade DEM extracted from UAV aerial photography along the eastern section. **(D)** Topographic profiles across portions of 1609 rupture traces.

the terrace will be higher as the number becomes larger in this study) attest to the tectonic activity in the area (Yang et al., 2020). Fault scarps are 20 and 40 m high on the terraces T5 and T6, respectively. These terraces were eroded by seasonal streams and slope flows, and consequently, these terraces developed new surfaces with different heights. There were distinct scarps detected on these new surfaces, except for the active surface, which remained submerged in water during seasonal streams flood. On the left bank of the Hongshuiba River, no structural scarp was found on the surfaces younger than T5 as the river gorge is about 400 m wide.

The preserved surface rupture on the Hongshuiba River site can be divided into two sections (**Figure 4A**). The western section starts by the river, and most of it strikes at approximately 125° with a total length of ca. 400 m. Two low scarps occur on the eroded slope of the large fault scarp of T5 near the river, and the vertical offset of the slope surfaces are 0.9 ± 0.1and 1.2 ± 0.1 m, respectively according to the profile by differential GPS (**Figure 4D**, Profile 14,019; **Supplementary Figure S1A**). The sharp parts of the scarps, composed of gravel, are 0.4 ± 0.1 and 0.7 ± 0.1 m high, respectively, which could represent the free faces caused by the most recent event (**Supplementary Figure S1A**). These two scarps merge into a simple fault scarp in the east. Additionally, it crosses the terrace of an ephemeral gully at point 14,022 with a vertical offset of 1.1 ± 0.1 m according to the profile by differential GPS (**Figure 4D**, Profile 14,022).

The eastern section is approximately 2 km long with a nearly E–W strike. It extends intermittently to the east, gapped by active gullies and alluvial fans. The scarps of this section present as one or two strips at different locations, and changes in their height range from 0.4 to 5 m on different surfaces, but values are mostly lower than 1 m for the scarps that occur on T1 of active gullies. Two traces of scarps occur at the western end of this segment. The northern scarp on T1 of active gullies is 0.4–0.7 ± 0.1 m high according to the profiles by tape and compass (Profile 160,609 in **Figures 4B,D**, photographs in **Supplemental Figures S1E,F**), and the height is 1.7 m on T2 according to the profile by differential GPS (Profile 14015P in **Figure 4D**, photograph in **Supplemental Figure S1F**). In trench Tc3 (location in **Figure 4A**), a south-dipping fault with a dip angle of 40° was revealed with a 1.5–1.7 ± 0.3 m vertical offset, measured by a laser distance meter (**Supplemental Figure S1G**; Huang et al., 2018b). According to this trench work, the most recent event occurred after AD 1. In the east part of this section, shifting scarps exist at some locations. The northern scarps are of the same height at approximately 0.7 ± 0.1 m, profiling by differential GPS, regardless of the location on T2 or T1 of the gullies, but a higher scarp is present only on T2 in the south (Profile 14,010 and Profile 141,012 in **Figure 4D**). Gravels are outcropped along the northern scarps (**Supplemental Figures S1B,D**). Along the trace of fault scarps, no obvious lateral landform offsets were found in the Hongshuiba River site.

The digital elevation model (DEM) extracted from UAV aerial photography agreed with the differential GPS profile results from our field work. For example, the offset of the young surface along the northern scarp on the eastern section ranged from 0.4 to 1.2 m according to the DEM (**Figures 4B,C**), and these data were in accordance with Profile 14,008 data produced by the differential GPS (**Figure 4D**).

Shiyangjuan Site

The Shiyangjuan surface rupture segment meets the Hongshuiba segment in its western portion. Its trace is very sinuous compared to the Hongshuiba segment, and it generally strikes 110°. Along the trace, the offset of terraces T1 in gullies is approximately 0.6–1.4 ± 0.1 m, according to the profiles extracted from the UAV DEM and the profiling data collected by tape and a compass. The results of these two profiling methods were in accordance with each other. At point 14,040 (*see* the scarp photographs in **Supplemental Figures S2B,C**), the vertical surface offset is 1.3 ± 0.1 m according to the DEM profile from the UAV aerial photography (**Figure 5C**, Profile 14,040), and it is 1.4 ± 0.1 m according to the tape and compass measurements. At point 14,042 (see the scarp photographs in **Supplemental Figures S2D**), the surface offset is 0.8 ± 0.1 and 0.6 ± 0.1 m, respectively, according to the two methods used (**Figure 5C**, Profile 14,042). Although the offset of terraces T1 has a wide range of 0.6–1.4 m, but most of these offsets are between 1.2 and 1.4 m except the local area around point 14,042 (**Figure 5B**). The small offset of point 14,042 may be caused by slip variation, or caused by the local severe erosion on the offset surface, especially while the length of the profile is obviously shorter than the other points, such as point 14,040. The T2 in small gullies were found to be vertically offset by approximately 1.6–2.0 m, with free faces on the scarps; for example, the surface offset is 1.9 ± 0.1 m at point 14,043 (Profile 14,043 in **Figure 5C**), and the free face was approximately 0.6 m high (**Supplemental Figure S2E**). The surface offset is larger on T2 in large gullies, for which the offset is approximately 4.5 ± 0.1 m at the stream outlet of the Shiyangjuan gully (**Figure 5C**), measured by the GPS profile and DEM profile, with a 0.7 ± 0.1 m high free face composed of large gravels (**Supplemental Figure S2A**).

Dalong River Site

The Dalong River site is located east of Shiyangjuan. The trace of the newest surface rupture of this segment is arcuate and NE extruding with a generally 122° strike; it presents as one or two strips of fault scarps. The vertical offset of T1 at the Dalong River across the trace is approximately 1.0–1.5 ± 0.1 m according to profiles.

In the area west of the Dalong River segment, a simple fault scarp occurs on T1 in a branch gully at point 14,182, and the vertical offset determined by differential GPS profiling is 1.5 ± 0.1 m (**Figure 6B**). This terrace is covered by conglomeratic sand without loess (**Figure 6C**). The loess is a common surface cover in the region and dated to the early Holocene. Therefore, this terrace should have formed much later than the loess deposition; its vertical offset is suggested to be related to the most recent earthquake. The 1.5 m offset is the maximum vertical offset of the most recent surface-ruptured event at this site. It is slightly larger than the offset measured on T1 in the East Shiyangjuan gully, west of the Dalong River site, where the value is 1.3 ± 0.2 m, and the age of that terrace is 2.8 ± 0.2 ka (Yang et al., 2017).

At point 14,199, the vertical offset of T1 along the eastern riverbank is 1.1 m, as measured by differential GPS profiling

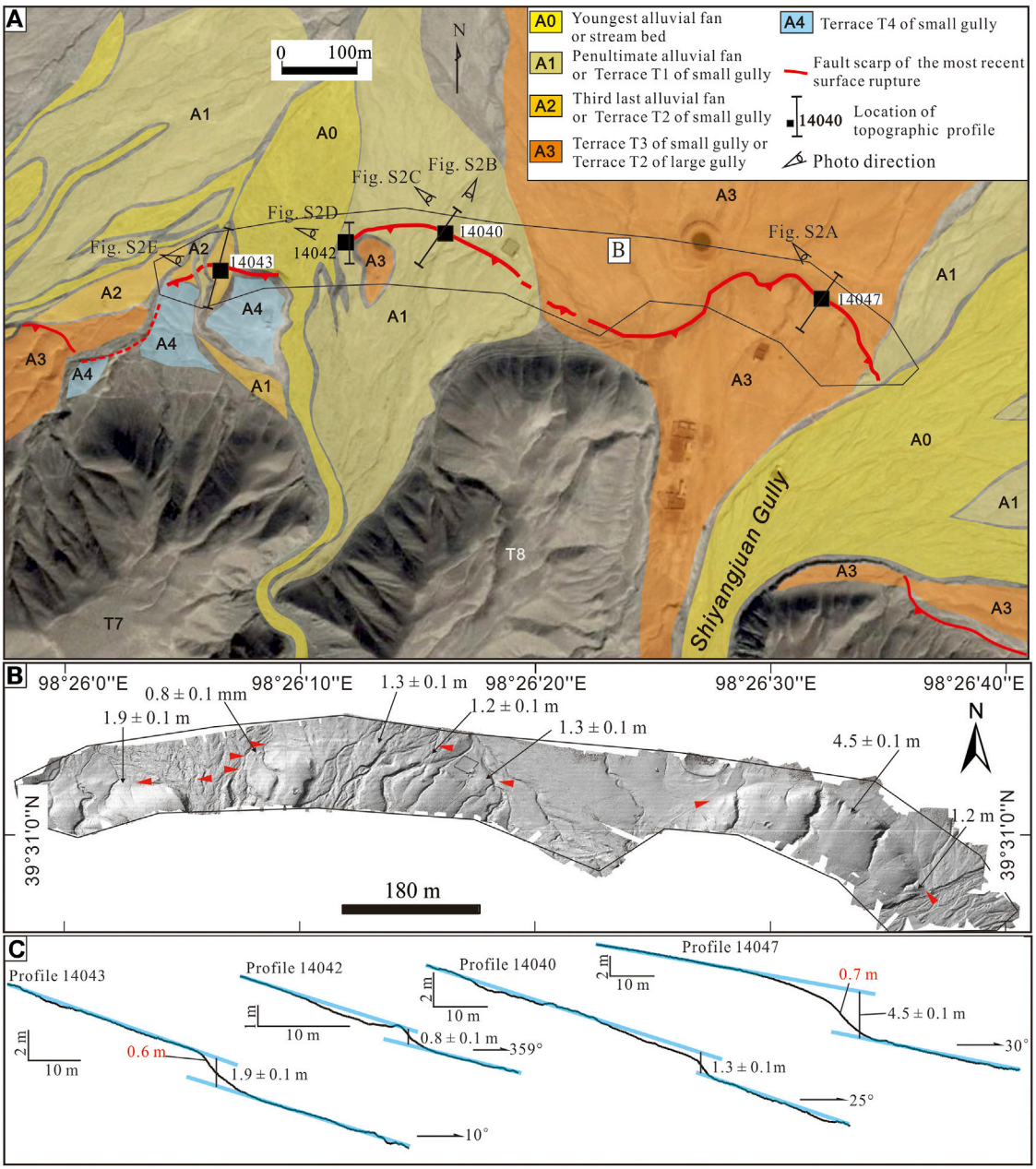

FIGURE 5 | Topographic features of the 1609 earthquake surface rupture at the Shiyangjuan site. **(A)** Surface rupture map **(B)** Hillshade DEM extracted from UAV aerial photography along the Shiyangjuan segment. **(C)** Topographic profiles across portions of 1609 rupture traces.

across a simple scarp (**Figure 6B**), and there is minimal loess cover on it (**Figure 6D**).

Fault scarps also occur on the terraces of the ephemeral gullies that flow to the north on T3 along the Dalong River. At point 14,197, the scarp on T2 in the gully is 3.5 ± 0.3 m high, and it is 0.4 ± 0.3 m high on T1 (**Figure 6E**).

Fengle River Site

The Fengle River site is located on the middle segment of the FHF. The fault scarps generally trend 80° at this site and turn to 120° in the eastern portion. The simple fault scarps occur on the T3, T4, and T5 terraces as a high escarpment in the estuary of the Fengle River (Yang et al., 2017). We found it difficult to recognize the fault scarps on T1 because of the severe artificial modifications here. However, some scarps have been preserved on the late erosional surface of T2, which adjoins the escarpment on the higher terraces.

The T2 along the river is covered by a thin layer of loess, and it has been dated as 6.0–7.3 ka on the west river bank (Yang et al., 2017). Gravels are outcropped here on the fault scarp. At point 14,081 (**Figure 7A,B**), the vertical offset is 2.7 ± 0.1 m (as determined by the differential GPS profile) across the scarp on T2 of the west river bank, and large gravels are present on the

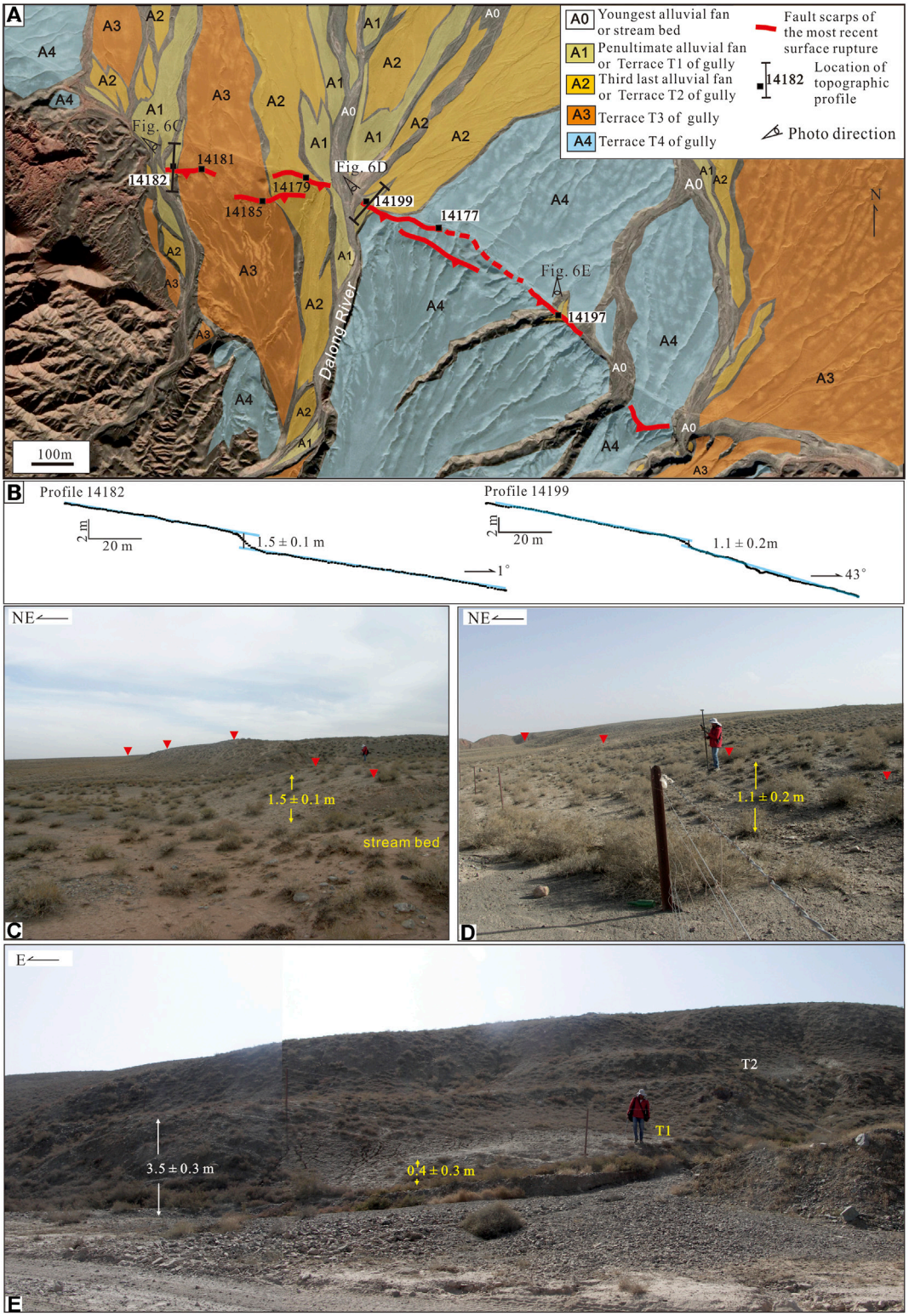

FIGURE 6 | Topographic features and photographs of the 1609 earthquake surface rupture on the Dalong River site. **(A)** Surface rupture map. **(B)** Topographic profiles across portions of 1609 rupture traces. **(C)** A simple fault scarp exists on T1 of a gully, covered by conglomeratic sand, and the vertical offset is 1.5 m. **(D)** The vertical offset of the first terrace of the Dalong River is 1.1 m across a simple scarp with low amounts of loess covering it. **(E)** Fault scarps are present on the terraces of ephemeral gullies on T3 of the Dalong River.

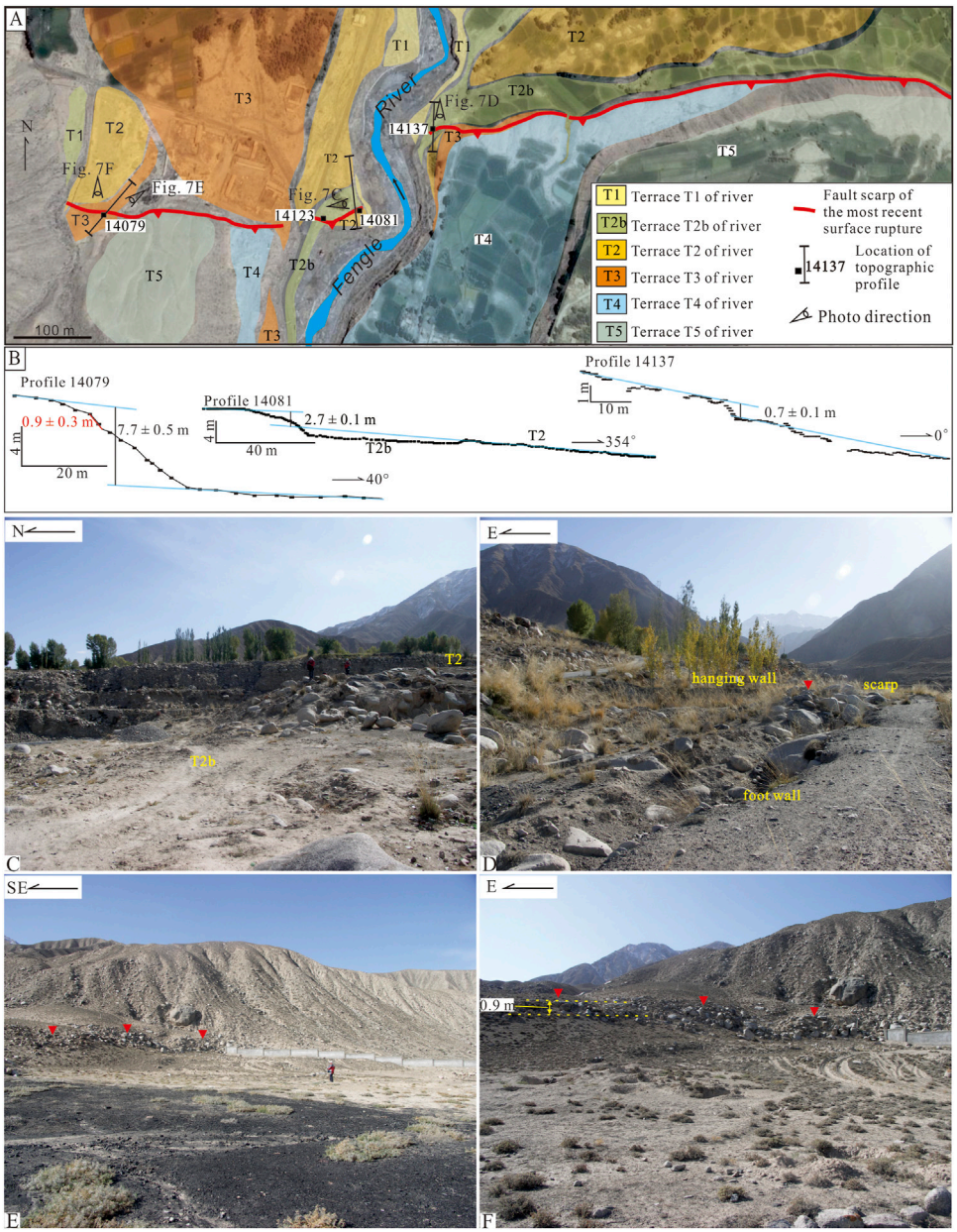

FIGURE 7 | Topographic features and photographs of the 1609 earthquake surface rupture at the Fengle River site. **(A)** Surface rupture map. **(B)** Topographic profiles across portions of 1609 rupture traces. **(C)** Gravels are outcropped on the fault scarp of T2 in the west river bank at point 14,081, and T2b is the late erosional surface on T2 with cobbles and gravels exposed. **(D)** A north-dipping scarp approximately 1.0 m high is present on T2b on the east river bank. **(E,F)** Free faces composed of boulders occur on high scarps of higher terraces on the west river bank, and the free face is approximately 0.9 m at point 14,079.

scarp (**Figure 7C**). Cobbles and gravels are exposed on the late erosional surface of T2 along the river, and north-facing scarps about 1.0 m high occur on this surface. The vertical offset of the surface is 0.7 ± 0.1 m at point 14,137, as measured by the differential GPS profile (**Figures 7B,D**). Free faces composed of boulders occur on high scarps of older terraces, including the late erosional surfaces on T5 along the west river bank (**Figure 7E**). The free face is approximately 0.9 ± 0.3 m at point 14,079, as measured directly by a laser distance meter (**Figure 7F**). No apparent lateral offset landform was found in this site. On its eastern portion, the vertical offset of the T1 terrace of a gully is 0.8 ± 0.3 m, measured by a laser distance meter, at point 169,085. And this value is similar to the vertical offset of the late erosional surface of T2 along the Fengle River.

Huangcaoba Site

The Huangcaoba site is located in the area east of the Fengle River, and this segment is also on the middle segment of the FHF. There are fault scarps of different heights on terraces in the river mouth of the Huangcaoba River, similar to the Fengle River site.

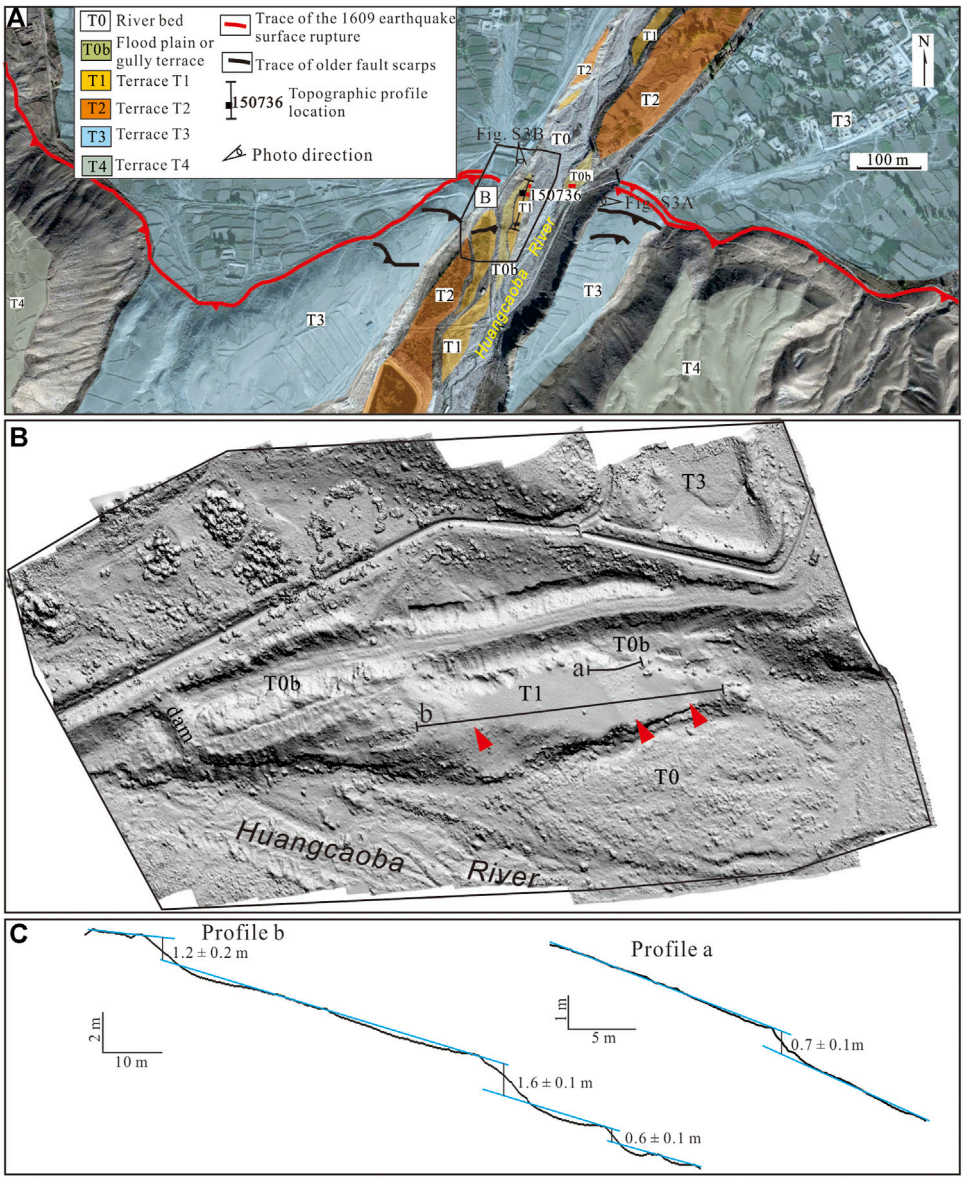

FIGURE 8 | Topographic features of the 1609 earthquake surface rupture at the Huangcaoba site. **(A)** Surface rupture map **(B)** Hillshade DEM extracted from UAV aerial photography of the estuary of the Huangcaoba River. **(C)** Topographic profiles across portions of 1609 rupture traces.

However, these constitute multiple scarps here and thus are different from the simple scarps at the Fengle River site.

According to the altitude differences compared with the river bed, we label the terraces in the river mouth area as T1, T2, and T3 from low to high. Four strips of fault scarps exist on T3, and these merge into a simple scarp toward the east or west (**Figure 8A**). T2 was not preserved along the fault trace because of later lateral washout and it was replaced by T1. Three fault scarps occur on T1 along the western river bank (**Figures S3A, 11B**), and UAV aerial photography was carried out here (**Figure 8B**). Vertical offsets were measured as 1.2 ± 0.2, 1.6 ± 0.1, and 0.6 ± 0.1 m from south to north on these scarps by extraction profiles from the DEM of the UAV aerial photography (**Figure 8C**). A small terrace was formed by an abandoned stream on the T1 terrace (marked as T0b in **Figures 8A,B**); this was displaced by the central fault and subsequently formed a 0.7 ± 0.1 m high fault scarp (**Figure 8C**). The excavation of the gully wall below the scarp, i.e., trench Tc4, revealed a south-dipping fault with an angle of 22°, which displaced the top of a gravel layer 1.5 ± 0.3 m vertically, measured by a laser distance meter (**Supplementary Figure S3C**). Two surface-ruptured events were found in Tc4, and the most recent event was dated as post-dating 1184–1275 AD, which is compatible with the rupture occurring in the 1609 event (Huang et al., 2018b).

Cobbles and boulders are exposed at the northern and middle scarps on the T1 terrace, but only small amounts of gravels are

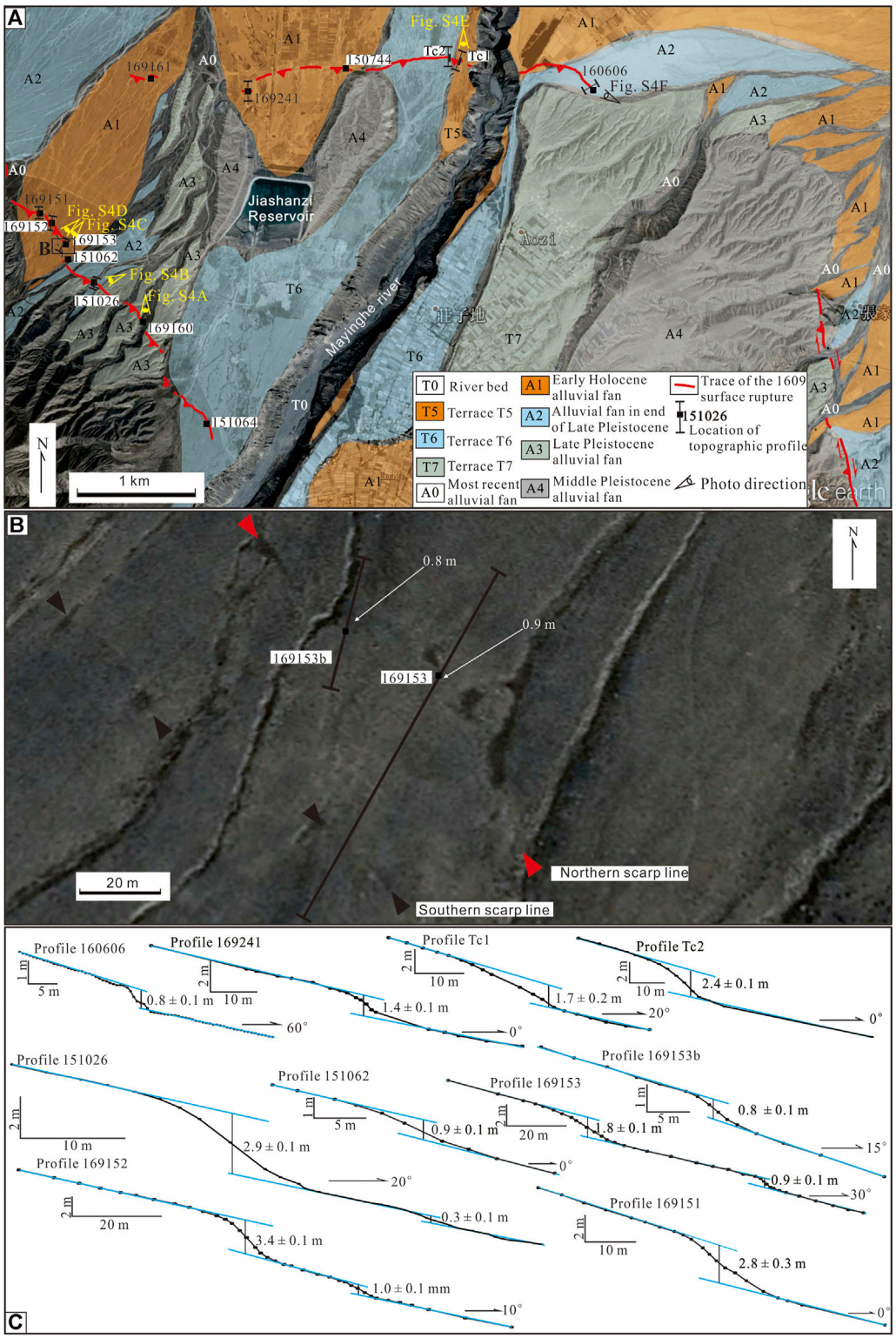

FIGURE 9 | Topographic features of the 1609 earthquake surface rupture on the Mingying River site. **(A)** Surface rupture map; the box near B shows the location of Figure **B**. **(B)** Detailed remote-sensing image from Google Earth showing the trace of the shifting scarps at point 169,153, SW of Jiashanzi. **(C)** Topographic profiles across portions of 1609 rupture traces.

outcropped at the southern scarp. We suggest that the fault breached the surface through the northern and middle scarps and did not break through the southern scarp during the most recent earthquake event. The most recent vertical offset revealed in Tc4 across the scarp on T0b is 0.7 ± 0.1 m; and it is about half of the vertical offset of the middle scarp of T1, which is 1.6 ± 0.1 m. Therefore, we suggest that at least half of the vertical offset across the north scarp on T1 could be caused by the most recent event and we cannot exclude the possibility that the whole scarp height could also be caused by this event. Then, the total vertical offset of this event at the Huangcaoba site is approximately 1.4 ± 0.3 m, while the total vertical offset at the northern and middle scarps ranges between 2.2 ± 0.2 and 2.5 ± 0.2 m (this study and Yang et al., 2016).

Maying River Site

The middle segment and east segment of the FHF adjoin at the Maying River site. The most recent rupture trace, located along the mountain front, mainly trends 125° in most places, but the trace turns to 140° on the west bank of the Maying River and stops near the river bank. No fault scarp was found on the river terraces near the mountain front on the eastern riverbank (**Figure 9A**).

Xu et al. (2010) assessed the outlet of Changcheng gully west of Mayin River, finding no evidence for the 1609 earthquake surface rupture on the youngest fans deposited during 0–3 ka, and they concluded that the 1609 rupture stopped at the Hujiatai anticline. We revisited the Changcheng gully and its surrounding area to made detailed field works in the west of the Maying River and found many surface rupture evidences in this area. Along the mountain front, west of the Maying River, low simple scarps approximately 1.0 ± 0.3 m high exist on young surfaces, such as the Late Holocene alluvial fans with gravels outcropped and no loess coverage, high flood plains of large gullies, and T1 terraces of ephemeral gullies. On the T1 terrace of Changcheng gully, a scarp is 1.2 ± 0.3 m high, measured by a laser distance meter, at point 169,146 (**Supplementary Table S1**). On the outlet of a large seasonal gully east of the Changcheng gully, the scarp at point 151,062 is 0.9 ± 0.3 m high, measured by tape and compass profile, on the high flood plain (Profile 151,062 in **Figure12B**), and the scarp at point 169,160 is 1.0 ± 0.3 m high, measured by a laser distance meter, on the T1 terrace of an ephemeral gully (**Supplemental Figure S4A**). Next to these small scarps, large simple fault scarps occur on the older and higher surfaces.

Shifting scarps are common in this section. These scarps have a large scarp in south and a small scarp in north, and the height of north scarp is similar with the scarp on youngest surface, which is supposed to occur in the most recent earthquake. At point 169,153, there are two scarps on T1 in a large seasonal gully, and the vertical offset on the southern scarp and northern scarp is 1.8 ± 0.1 and 0.9 ± 0.1 m, respectively, as measured by tape and compass profiling (location shown in **Figure 9A**, profile presented in **Figure 9B**, and photograph presented in **Supplemental Figure S4C**). Along the strike of the northern scarp on T1 (**Figure12B**), a scarp with a vertical offset of 0.8 ± 0.1 m occurs on a small ephemeral gully terrace lower than T1 (Profile 169153b in **Figure12C**; **Supplemental Figure S4D**), but no scarp occurs on this lower terrace along the strike of the southern scarp on T1. Furthermore, the vertical offsets of the southern scarp and northern scarp are 3.4 ± 0.1 and 1.0 ± 0.1 m, respectively, at point 169,152, and values are 2.9 ± 0.1 and 0.3 ± 0.1 m, respectively, at point 151,026, all measured by tape and compass profiling (**Figure12C**; **Supplemental Figure S4D**).

Xu et al. (2010) found no evidence of deformation of the Hujiatai anticline during the AD 1609 earthquake by mapping on the aerial photos and in the field. We did detailed field observation and found a 5 km long fault scarp along the north-limb of the Hujiatai anticline (Yang et al., 2018b) in the area north of the Jiashanzi Reservoir at the Maying River site. It starts in northwest of Jiashanzi and extends to the east along the eastern bank of the Maying River with a nearly E–W strike, proving the western end of the eastern rupture segment reached Maying River area in the AD 1609 earthquake. The most robust evidence comes from our trenching work across the fault scarp on the T5 and T6 terrace of the western riverbank. In trench Tc1 across the 1.7 ± 0.2 m high scarp on the T5, south-dipping faults with a dip angle of 22–25° and two surface-ruptured events were revealed. The most recent event was considered as the 1,609 earthquake, and the vertical offset caused by it is approximately 0.7 ± 0.3 m (**Supplemental Figure S4G**, Huang et al., 2018b). The fault scarps on the T6 terrace are approximately 2.2–2.6 ± 0.2 m high, measured by tape and compass profiling. Three surface-ruptured events were revealed in the trench Tc2 across the fault scarp, which is approximately 2.2–2.4 ± 0.3 m vertically offset totally. Based on the trench work, we suggest that the vertical slip of the 1609 earthquake was approximately 0.7 ± 0.3 m on T5 and T6 (Huang et al., 2018b). Apart from the river, fault scarps turned out to be lower. In the area northwest of Jiashanzi, a low scarp approximately 0.8 ± 0.3 m high, measured by a laser distance meter, with a length of 300 m occurs on the terraces of ephemeral gullies and young fans. Additionally, at the eastern end of this section, i.e., point 160,606, the vertical offset of the surface is approximately 0.8 ± 0.1 m by tape and compass profiling (Profile 160,606 in **Figure 9C**). Therefore, according to the above-mentioned findings, the vertical offset of the 1609 earthquake is 0.7–0.8 ± 0.3 m along the Maying River section of the eastern segment of the rupture.

Vertical Fault Slip Along the FHF

West Segment

According to our detailed field work, the 1609 earthquake surface rupture can be divided into three main geometric segments separated by important steps, similar to the previous segmentation of the FHF (Yang et al., 2017). In the Hongshan Village (HSC), the western segment and middle segment are separated by changes in rupture trace orientation and dip angles (**Figure 10A**), and on the western bank of the Maying River, the middle segment and eastern segment are separated by a ~5 km wide step (**Figure 11B**). We obtained 94 offset data points during our field work, and most of these data consisted of vertical offsets with an average of 1.0 ± 0.3 m.

The west segment of the 1609 surface rupture trends 115° from Fodongmiao to Hongshancun, with a length of ca. 24 km. The separation demarking the middle segment is a small section of fault trending 73°, with a length of approximately 2.5 km; sinistral

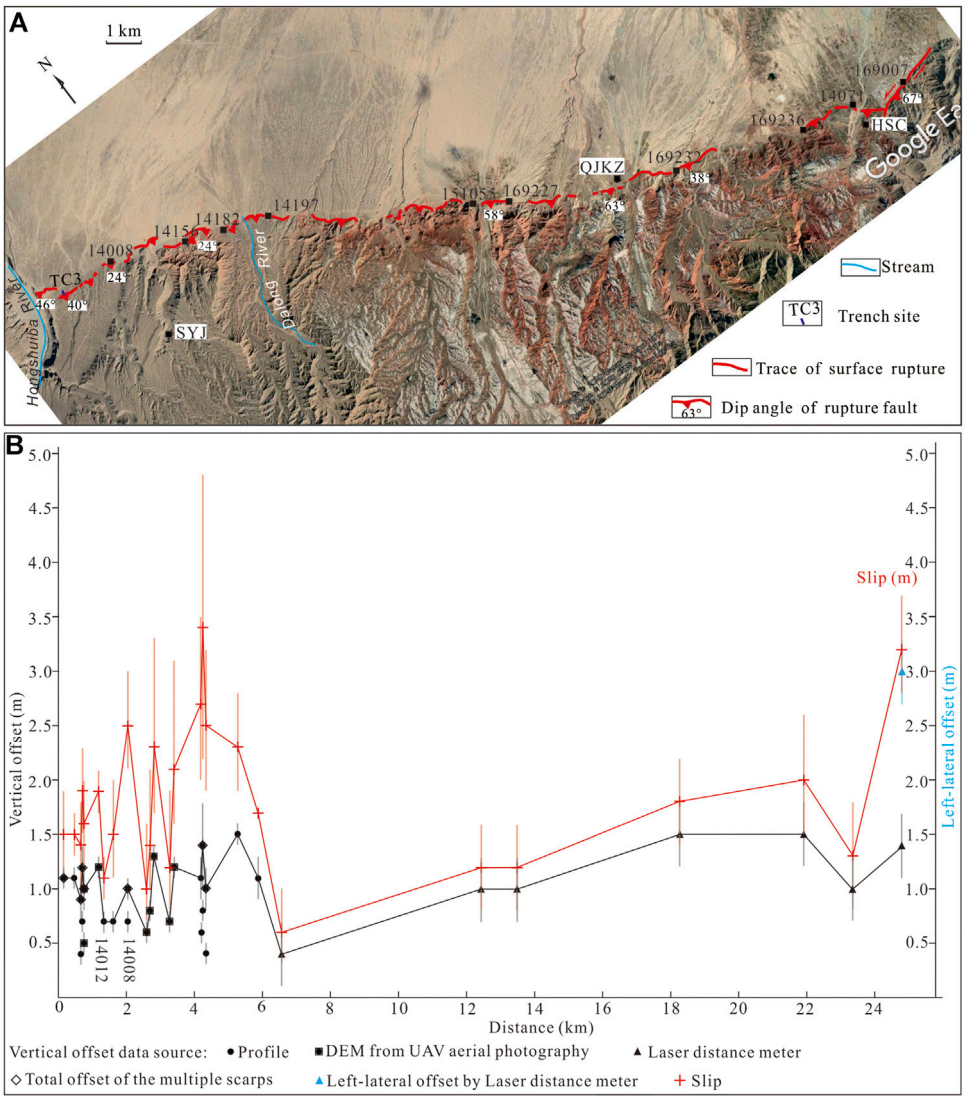

FIGURE 10 | (A) Map of the 1609 surface rupture in the western segment. Place names: SYJ, Shiyangjuan; DLH, Dalong River; QJKZ, Qujiakouzi; HSC, Hongshan Village. **(B)** Offset and slip of the 1609 earthquake in the western segment.

offsets were measured at a few locations on it, in the area east of the Hongshancun. And these Left-lateral offsets are compatible with the change in strike as the rupture accommodating a NE-directed slip vector. Although the trace is sinuous in some locations such as the Shiyangjuan site, most of the rupture trace in the west segment is relatively straight compared with that in the middle and eastern segments. The majority of the interruptions of the trace were caused by active gullies, rivers, and alluvial fans, but the existence of some stepovers with a width of 200–300 m was also noted, such as along the trace on the Hongshuiba River sections. The preserved surface rupture in the west segment consisted of mostly simple fault scarps, and part of them contained multiple scarps or shifting scarps with two or three strips. The spacing between the two strips is generally less than 100 m, but values can reach 200 m locally. Most of the fault planes breaching the surface are south-dipping with a dip angle of 40°, as revealed by the profiles of trenches and gullies.

The vertical slip of the 1609 earthquake was acquired by measurement of the surface offset on the young surface or by measuring the shifting scarps on T1 in large gullies and T2 in small gullies; a few data points were estimated via the heights of free faces. According to the results, average surface offsets are approximately 1.0 ± 0.3 m with a reliable maximum of 1.5 ± 0.3 m in the western segment (**Figure 10B**; and **Supplementary Table S1**). The maximum of the surface offsets occurs at the Dalong River site, east of Qujiakouzi and west of Hongshancun. It was obtained by differential GPS profiling at the Dalong River site, and the value was approximated by the scarp height measurements taken via a laser distance meter at the remaining two locations.

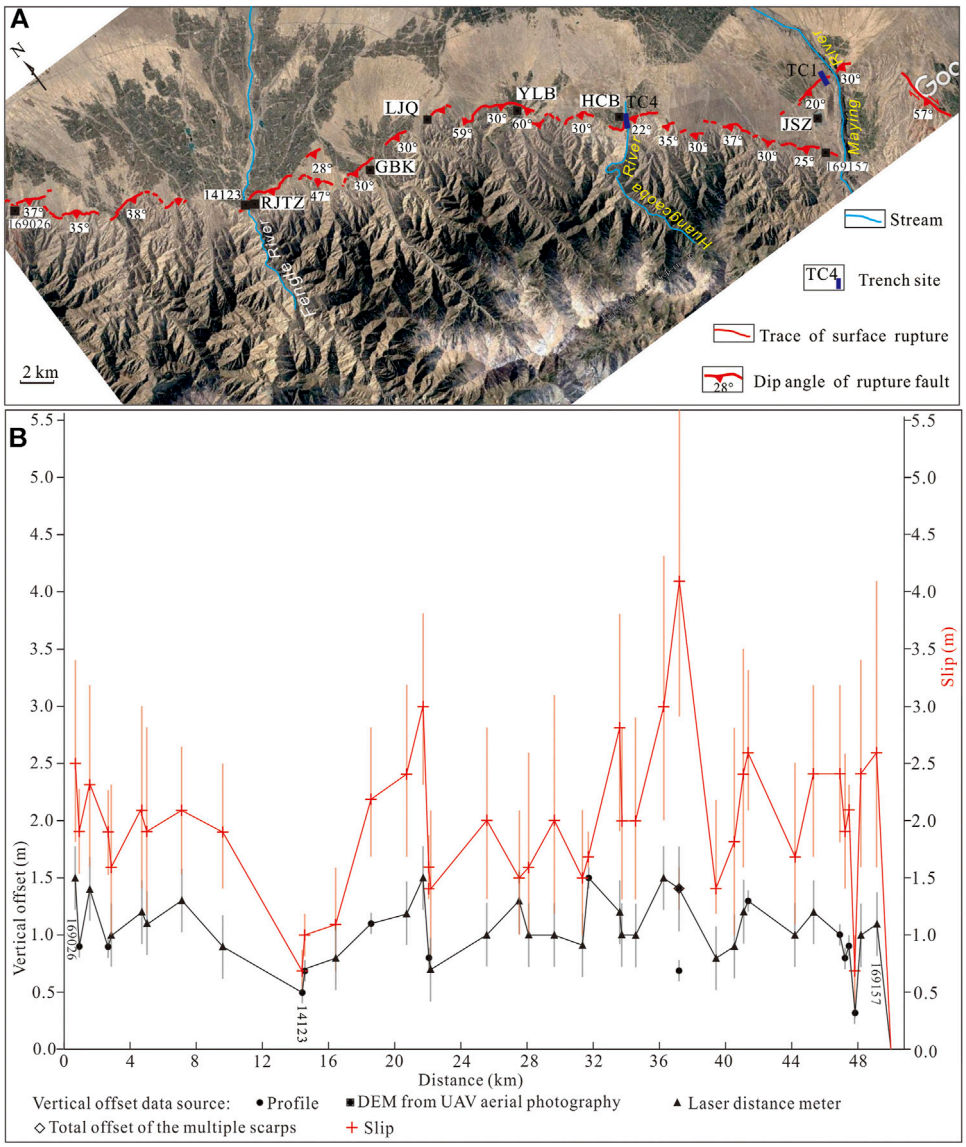

FIGURE 11 | (A) Map of the 1609 surface rupture in the middle segment. Place names: JFS, Jinfosi; GBK, Ganbakou; LJQ, Luejiaquan; YLB, Yulinba; JSZ, Jiashanzi. **(B)** Offset and slip of the 1609 earthquake in the middle segment.

The surface rupture was almost completely vertically offset with a sinistral motion noted only in that area east of Hongshancun, where the fault strike is rotated about 45° counterclockwise relative to the overall thrust geometry. At point 169,007, the north-dipping scarp on T1 in the gully is approximately 1.0 ± 0.3 m high, as the riser of T1 is left-lateral offset 3 ± 0.3 m, as measured by a laser distance meter. We take these data as the most recent offsets with some uncertainty. Because hanging wall of this scarp was badly eroded, the measured vertical offset could be underestimated. And the lateral offset may also include multiple events as we did not have any dating data of this terrace. Except for Hongshancun, no obvious larger landform offsets along the field traces were indicative of horizontal motion, and we suggest the lateral slip is purely a geometric effect, not a large-scale kinematic change.

We divide the vertical offset by the sine of the dip angle to get the dip slip and take it as the slip where no lateral offset exists. If there is lateral offset, we sum up the square of the dip slip and the square of the lateral offset, and take the square root of the sum as the slip. We converted the vertical offsets to dip slip using dip angles of rupture faults revealed in trenches and gullies for the majority of the data, but chose a neighbor dip angle for the points without outcropped fault plane (**Figure 10B**; **Supplementary Table S1**). And it will bring in some uncertainties as we are not sure if the local dip angles can change a lot in short distance along the fault strike. The maximum slip in the western segment is 3.4 + 1.4/−1.2 m in

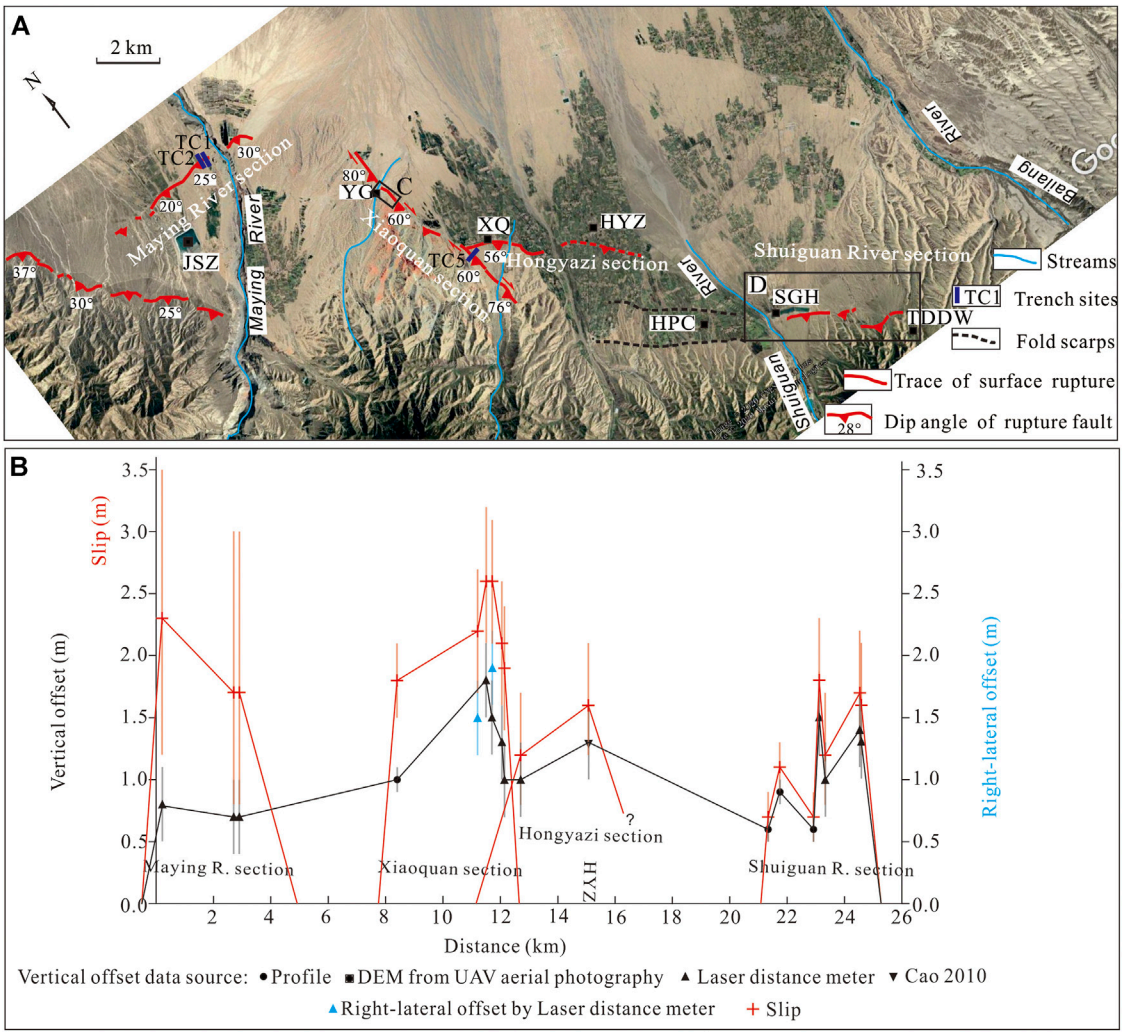

FIGURE 12 | (A) Map of the 1609 surface rupture in the eastern segment. Place names: JSZ, Jiashanzi; YG, Yagou; XQ, Xiaoquan; HYZ, Hongyazi; HPC, Heping Village; SGH, Shuiguan River reservoir; TDDW, Toudaodongwan. **(B)** Offset and slip of the 1609 earthquake in the eastern segment. Only one right-lateral offset data point, measured beside Tc5 in the area south of Xiaoquan, is plotted because the locations of the measurements were close and the data range was narrow around 1.5 m.The box signed **C** is the location of **Figure 13A**, and the box signed **D** is the location of **Figure 13B**.

the east of Shiyangjuan (SYJ in **Figure 10A**) and average slip is 1.8 + 0.6/−0.5 m (N = 29).

Because the youngest surfaces relevant to ruptures have slope angles mostly smaller than 5°, the vertical offset of the surfaces is close to the vertical slip of the rupture, so we take the vertical offset as the vertical slip to calculate the dip slip of the rupture. But in turn this calculation will bring some overestimate of the slip because the vertical offset is a little larger than the vertical slip.

Middle Segment

The middle rupture segment trends 120° from the area east of Hongshancun to the west bank of the Maying River, with a length of ca. 50 km. The rupture trace is sinuous and mainly northeast protruding arc-shaped; the arc top is located between the villages of Luejiaquan and Yushuba (**Figure 11A**). The easternmost of the middle segment turns to a 140° strike and is distributed along the mountain front in the area southwest of Jiashanzi along the western bank of the Maying River.

The segment is composed of dozens of small sections of ruptures of different lengths amounting to several hundreds of meters or kilometers. Most of the small sections are distributed along the mountain front, and a few of these are present on alluvial fans hundreds of meters or even kilometers away from the mountain front. These sections are separated by stepovers with a width of hundreds of meters, or by Holocene alluvial fans without a rupture trace. Compared to the west segment, the rupture trace in the middle segment is more sinuous and zigzag. The fault plane of the surface rupture is south-dipping at 35 + 27/−15° dip angle in average with a range from 22 ± 2° to 60 ± 2° as revealed in the profiles of trenches and stream banks.

Average surface offsets are also approximately 1.0 ± 0.3 m with a reliable maximum of 1.5 ± 0.3 m in the middle segment (**Figure 11B**; **Supplementary Table S1**). The maximums of the surface offsets are located between the area east of Hongshan village and the Huangcaoba River site. The maximum value at the Yulinba was obtained by tape and compass profiling, and the remaining data were measured directly by a laser distance meter on the scarp height.

The surface rupture was completely reverse-sense without obvious landform offsets along the field traces indicating horizontal motion in the middle segment. We converted the vertical offsets to dip slip using the fault dip revealed in trenches and stream banks and chose neighbor dip data to be substitutes for the points without outcropped fault plane (**Figure 11B**; **Supplementary Table S1**). The maximum slip in the middle segment is 4.1 + 1.4/−1.2 m in Huangcaoba (HCB in **Figure 11A**), and the average slip is 2.0 + 0.7/−0.6 m (n = 43).

East Segment

NNW-Trending Xiaoquan Oblique Dextral Fault Segment

The east segment of the 1609 surface rupture trends mainly 130° with a length of ca. 25 km from the Maying River to the Toudaodongwan. It is composed of four sections with different strikes. The westernmost section, i.e., the Maying River section, occurs on both sides of the Maying River and traces the north-limb of the Hujiatai anticline, north of Jiashanzi, with a total length of 5 km. The Xiaoquan section is near N–S trending from Zhangjiaquan to the area south of Xiaoquan, and it is 11 km long. The Hongyazi section joins the Xiaoquan section at a location west of Xiaoquan village and trends eastwards with a 130° strike; it stops on the west bank of the Shuiguan River and is ca. 5 km long (Xu et al., 2010). The easternmost section, i.e., the Shuiguan River section, trends 120° from the east bank of the Shuiguan River to Toudaodongwan, and it is 3.6 km long in total. This section is composed of three smaller sections with two stepovers of 200 and 600 m width, respectively.

The Maying River section of the rupture is completely vertically offset. The average surface offsets are approximately 0.7 ± 0.3 m according to the measurements on the terraces of small gullies and the layer offsets in trenches. Additionally, the fault planes of the rupture are south-dipping at 20–30°.

Along the Xiaoquan section, N15°W trending scarps occur on various surfaces except active fans and gullies. The fault strike is rotated about 45° clockwise relative to the overall thrust geometry and the NE slip vector could decompose into NEE compression and NNW lateral slip to show a right-lateral strike-slip sense along this fault section. In fact, the N15°W trending surface rupture shows both vertical and horizontal (right-lateral) offsets, compatible with the same slip vector with the whole fault. The vertical surface offsets range between 1.0 ± 0.1 and 1.8 ± 0.3 m (**Figure 12B**; **Supplementary Table S1**). The maximum vertical offset of 1.8 ± 0.3 m was measured directly on the scarp by a laser distance meter in the area south of Xiaoquan village. The right-lateral offsets were measured by a laser distance meter on the displaced gullies and terrace risers along the surface rupture trace. In the area west of Xiaoquan village, most of the small deflected gullies at the foot of the hill are right-laterally displaced by ca. 1.5 ± 0.3 m (Yang et al., 2018b; **Supplementary Table S1**). Vertical offset of 1.0 m was measured for the profile on T1 at Yagou (Duck gully) (**Figure 13A**; **Supplementary Figure S5A**), with minimal loess coverage, which are findings suggestive of having been caused by the 1609 earthquake (Xu et al., 2010). The T2 is vertically offset is 1.8 ± 0.3 m, and the T3 terrace riser is right-laterally displaced 2.3 ± 0.3 m (**Supplementary Figure S5B**).

Because of severe artificial reformation on the surface, it was difficult to obtain reliable rupture offsets along the Hongyazi section. We measured the scarp height of a small gully east of Xiaoquan village as being about 1.0 ± 0.3 m. This value is in accordance with that of a previous study, in which the range of scarp height caused by the 1609 earthquake was reported to be between 0.7 and 1.5 m (Cao, 2010; Xu et al., 2010). Two traces of fold-scarps with gentle slopes occur on the late Pleistocene alluvial fans in the area south of the Hongyazi fault scarp section, in Heping village (HPC in **Figure 12A**). No fault was found in the stream bank profiles across the fold-scarps, and their relationship to the 1609 earthquake remains unknown.

The surface rupture was completely dip-slip without lateral motion in the Shuiguan River section. In the area east of the Shuiguan River, fault scarps occur on T4 of the river, the hill slope, and the T1 and T2 terraces of gullies on the piedmont. Additionally, the heights of scarps range from 0.5 ± 0.1 to 4.5 ± 0.3 m. According to the locations and shapes of scarps, the scarps with a height of 0.5 ± 0.1–1.4 ± 0.3 m are suggested to have formed during the 1609 earthquake, but there remains a lack of age dating constraints.

Average vertical surface offsets of the east segment are approximately 1.0 ± 0.3 m as estimated with 16 sets of data (**Figure 12B**; **Supplementary Table S1**), and the average dextral offsets are approximately 1.5 ± 0.3 m as estimated with six sets of data from the Xiaoquan section (**Supplementary Table S1**).

Because the dip of the fault revealed in the trenches and outcropped on different sections are not the same and the motion senses are different, we converted the surface offsets of different sections into dip slip with different fault dips. The vertical offsets on the Maying River section were converted to dip slip by using fault dips as revealed in trenches Tc1 and Tc2, and drainage channels (Huang et al., 2018a; Huang et al., 2018b). The vertical and right-lateral offsets on the Xiaoquan section were converted to dip slip by using fault dip revealed in gully banks and the trench Tc5 (Huang et al., 2018b). We used a vertical offset average of 1.4 ± 0.3 m for the conversion of the right-lateral offset data measured beside Tc5 in the area south of Xiaoquan as there were no measurements of vertical offsets on these scarps. Additionally, vertical offsets without lateral offset data were converted to dip slip with a lateral offset average of 1.5 ± 0.3 m. The vertical offsets on the Hongyazi section and Shuiguan River section were converted to dip slip with a fault dip of 56 ± 5° from Tc-X, west of Xiaoquan village (Xu et al., 2010). The maximum slip in the eastern segment is 2.6 ± 0.5 m in the south of Xiaoquan and average slip is 1.8 ± 0.4 m (N = 22) (**Figure 12B**; **Supplementary Table S1**). Because all of the lateral offsets and most vertical

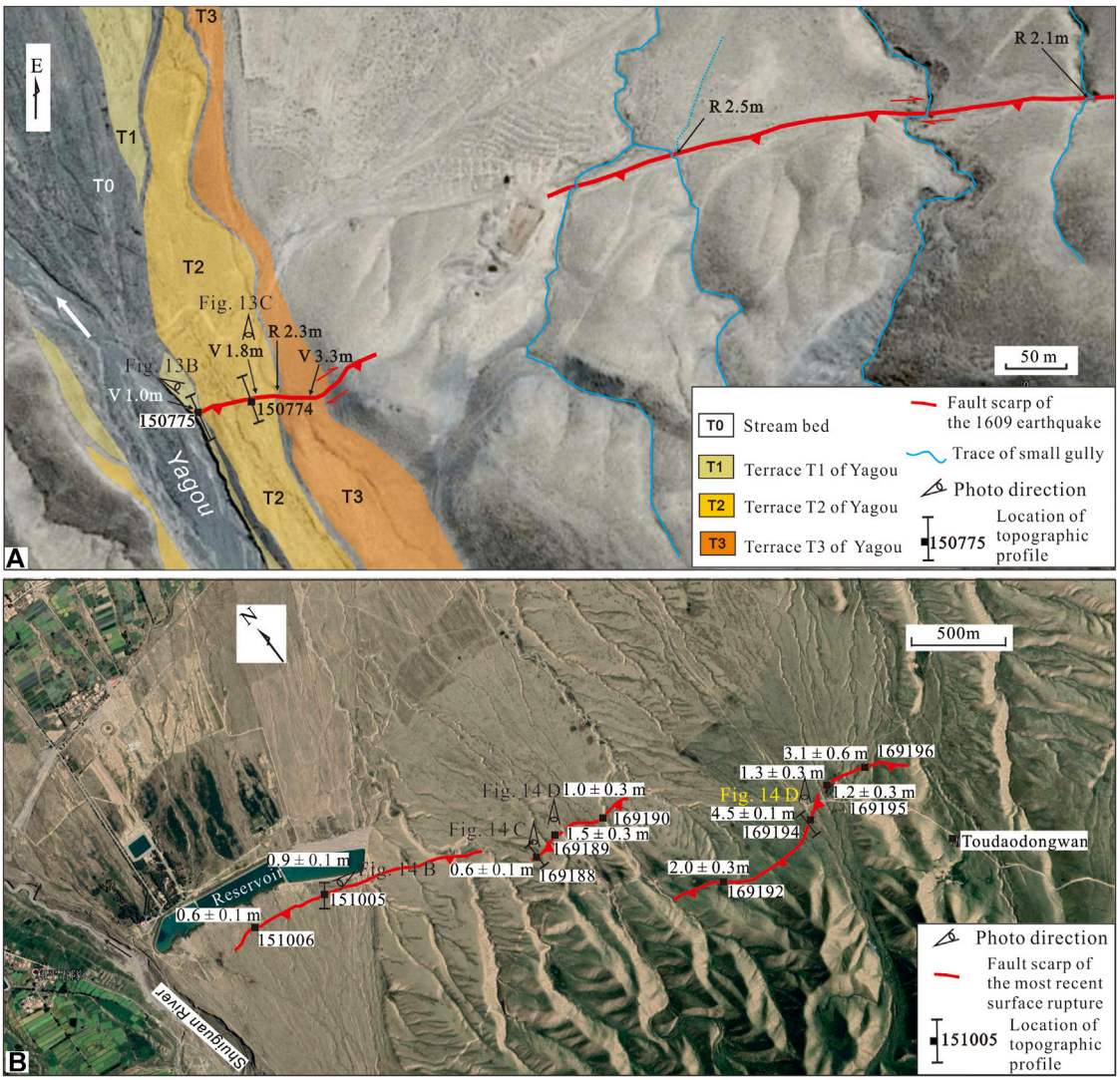

FIGURE 13 | Surface rupture maps of the 1609 earthquake on the Yagou site **(A)** and Shuiguan River section **(B)**.

offsets were sourced from direct laser distance meter measurements with an error of 0.3 m and the fault dip angles are only confirmed by a few trenches with some uncertainty, the slip data may include more uncertainty compared with other segments.

Shuiguan River Section

The surface rupture of the Shuiguan River segment can be divided into three small sections. The western one starts at the T4 terrace on the eastern bank of the Shuiguan River and extends to the hillslope in the east as linear scarps striking 116° with a total length of ca. 1.4 km. The T4 terrace of the Shuiguan River is covered by 1.5 m thick loess, and there is a gravel layer on top at some locations, which was caused by the accumulation of seasonal slope runoff. The vertical offsets of the T4 surface range from 0.6 ± 0.1 to 0.9 ± 0.1 m across the scarp, where values become lower from east to west (**Figure 13B**; **Supplemental Figure S6A**). Additionally, the surface offset on the hillslope in the east is approximately 1.2 m.

The middle small section has a sinuous trace striking 105° generally, with a total length of approximately 600 m. The separation between this section and the western one is approximately 200 m. In the westernmost portion of this section, a low scarp occurs on the hillslope and is covered by thick loess, where the vertical offset of the surface is 0.6 ± 0.1 m as measured by tape and compass profiling (**Supplemental Figure S6C**). Along the rupture trace, fault scarps are 1.0–1.5 m high as measured by a laser distance meter on gullies terraces (**Figure 13B**; **Supplemental Figure S6C**).

The eastern small section has an S-shaped trace trending 105° generally with a total length of approximately 1.4 km. A 600 m wide stepover occurred between the middle section and small section. Most ruptures are simple fault scarps, and only a few locations contain shifting scarps. The vertical offsets across the trace of simple fault scarps are 2.0–4.5 m. At point 16,194, in the area west of

Toudaodongwan, a composite scarp occurs on T2 of the gully and the total vertical offset is 4.5 ± 0.1 m according to tape and compass profiling (**Supplemental Figure S6D**). The steepest slope section of this scarp is approximately 1.4 m high, and this is in accordance with the scarp height on gully terraces on the middle section. To its east, this single scarp turns into two strips of scarps on the T1 terrace of another gully. The northern scarp is 1.3 ± 0.3 m high, and the southern one is 1.2 ± 0.3 m, measured by a laser distance meter. These are suggested to represent shifting scarps.

As mentioned above, the vertical offsets of the young surfaces on the Shuiguan River segment range from 0.6 ± 0.1 to 1.5 ± 0.3 m, and the maximum of 1.5 ± 0.3 m was measured directly from the height of the scarp determined by a laser distance meter on the T1 terrace of a gully. There are no age dating constraints on the surfaces to prove that these were from the 1609 rupture. However, at point 169,188, the scarp on the hillslope is low, about 0.6 m high, and it is preserved on a thick loess covered surface with a relatively steep slope (**Supplemental Figure S6B**). Under such conditions, old scarps can retreat and disappear after thousands of years (Zhang et al., 1994), so we are prone to consider the Shuiguan River segment as part of the 1609 surface rupture.

DISCUSSION

Rupture Length, Coseismic Slips, and Possible Magnitude of the 1609 Earthquake

As mentioned above, the west segment of the 1,609 surface rupture trending 115° from Fodongmiao to Hongshancun is ca. 24 km long, and the average and maximum slip is 1.8 + 0.6/−0.5 and 3.4 + 1.4/−1.2 m, respectively. The middle segment trending 120° from the area east of Hongshancun to the west bank of the Maying River is ca. 50 km long, and the average and maximum slip is 2.0 + 0.7/−0.6 m and 4.1 + 1.4/−1.2 m, respectively. The east segment trending generally 130° from the Maying River to the Toudaodongwan is ca. 25 km, or 17 km long not including the Shuiguanhe section, and the average and maximum slip are 1.8 ± 0.5 and 2.6 ± 0.5 m, respectively. The average and maximum slip of the whole rupture are 1.9 + 0.6/−0.5 and 4.1 + 1.4/−1.2 m, respectively.

The relation between the seismic moment (M_o) and the moment (Mw) magnitude is described by Hanks and Kanamori (1979) as follows:

$$Mw = (\log_{10} M_o - 9.1)/1.5 \quad (1)$$

Seismic moment can be calculated as the slip × area × rigidity (3.3×10^{10} Nm^{-2}). To estimate the moment from each fault segment, we used its mapped length and a dip of 30°, as adopted from previous studies on the seismic reflection profiles across the FHF (Yang et al., 2007; Zuza et al., 2016), along with an assumption of a 10 km seismogenic thickness because the estimated detachment depth of the FHF ranges between 6 and 15 km (Yang et al., 2007; Zuza et al., 2016) to compute the rupture area of the fault. The seismic moment estimates for the western segment, middle segment, and eastern segment are 2.85×10^{19} Nm, 6.60×10^{19} Nm, and 2.97×10^{19} Nm (or 2.02×10^{19} Nm not including the Shuiguan River section), respectively. Summing these three segments, we estimate that the total seismic moment was 1.24×10^{20} Nm (Mw 7.33), or 1.15×10^{20} Nm (Mw 7.30) not including the Shuiguan River section. On the west and east segments, most of the local slips are estimated based on local rupture dips steeper (or shallower) than 30° dip, based on which the area is calculated in the **Eq. 1**. This probably introduces some incompatibility. If local dip is 40° higher or 10° lower than regional dip (30°), then slip is 0.9 m smaller or larger, and the effect on the magnitude is + or −0.1. The change in dip doesn't change the magnitude estimate too much.

The total length of the surface rupture measured on the map is 98 or 90 km without the Shuiguan River section, and this length is slightly shorter than the sum of each segment because a stepover exists between the middle and eastern segments. We can assess the magnitude from the rupture length by using the empirical relation between the rupture length and magnitude for dip-slip faults, given by Leonard (2010), as follows:

$$Mw = 1.52\log_{10}(SRL) + 4.40 \quad (2)$$

Here, SRL is the rupture length. According to **Eq. 2** calculations, the predicted magnitudes are Mw 7.43 and Mw 7.37 for the 98 km and 90 km rupture lengths, respectively.

We also estimated the magnitude of the AD 1609 earthquake by another empirical equation from Wells and Coppersmith (1994), in which the relationship between the maximum displacement and magnitude is as follows:

$$Mw = 6.81 + 0.78\log_{10}(D_{max}) \quad (3)$$

Here, D_{max} is the maximum coseismic slip; this value is 4.1 + 1.4/−1.2 m at point 150,736 on the middle segment. According to **Eq. 3** calculations, the predicted magnitude is Mw 7.3 ± 0.1.

Implications for Thrust Fault Rupture Segmentation

Most of the recent rupture along the FHF could be traced on different surfaces, but the youngest ruptured surfaces on different segments are all from the Late Holocene. The most recent surface rupture on the western segment occurred after AD 1, which was proven by trench Tc3 data collected at the Hongshuiba River site (Huang et al., 2018b). The newest surface rupture on the middle segment formed after AD 1184–1275, as revealed by Tc4 data from the Huangcaoba site (Huang et al., 2018b). The most recent surface rupture on the eastern segment, which trends from the area west of the Maying River to the area west of the Shuiguan River, occurred in AD 1609, as proved by trench Tc1 and Tc2 data from the Maying River site (Huang et al., 2018b), as well as trench TcX data from Xiaoquan village (Xu et al., 2010). Jiuquan city, which is just 24 km south of the Hongshuiba River site, was built in 160 BC. during the Han Dynasty. Among the earthquakes included in the Chinese historical earthquake catalog (Li, 1960; Gu, 1983; Earthquake Disaster Prevention Department, State Seismological Bureau, 1995) and the China Earthquake Networks Center, 2020 (http://www.ceic.ac.cn/history), only the AD 1609 $M7^1/_4$

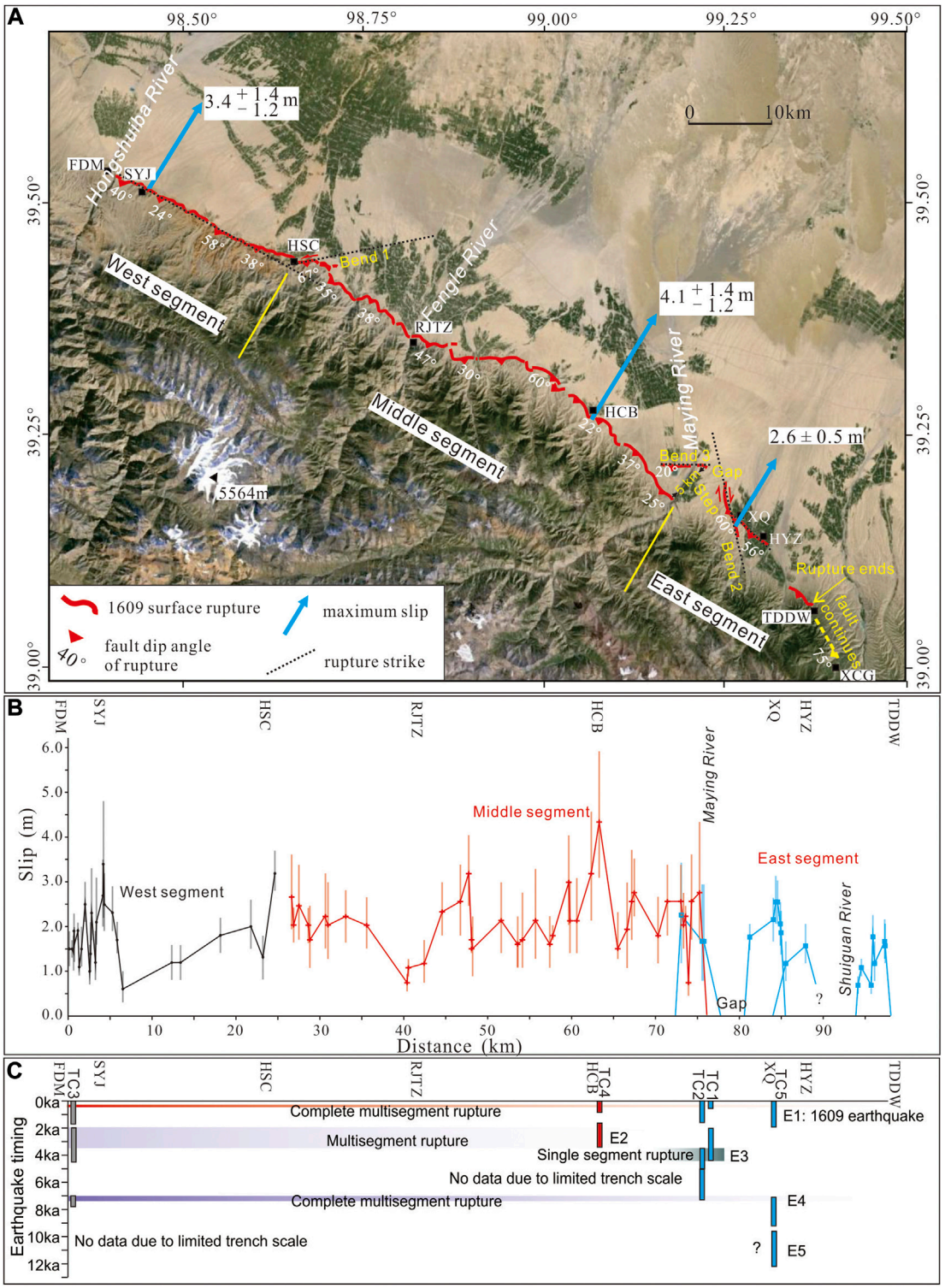

FIGURE 14 | Surface slip distribution of the 1609 earthquake and segmentation of surface rupture. **(A)** Surface rupture map and segmentation of the rupture. **(B)** Surface rupture slip distribution. **(C)** Possible correlation of the paleo-earthquakes along the Fodongmiao-Hongyazi Fault according the previous trenches work (Huang et al., 2018b). Place names: FDM, Fodongmiao; SYJ, Shiyangjuan; HSC, Hongshan Village; RJTZ, Rujiataizi; HCB, Huangcaoba; XQ, Xiaoquan; HYZ, Hongyazi; TDDW, Toudaodongwan; XCG, Xichagou.

Hongyapu earthquake could have been responsible for the most recent surface rupture running from the Hongshuiba River to the Shuiguan River. Therefore, the three segments of the FHF are considered to have coalesced and ruptured simultaneously during the AD 1609 earthquake, occurring as a multisegment rupture. This multisegment rupture event happened about 400 years ago, so the probability of large earthquakes along the FHF in the next 100 years is small, with consideration of the millennial-scale recurrence revealed in the trenches (Huang et al., 2018b).

In Hongshan Village (HSC), from the western segment to an oblique thrust fault striking 73°, the surface rupture trace orientation differs by about 42°, named as Bend 1 in **Figure 14**, and dip angles change from 38° to 54–78°. Structural discontinuities may indicate a rupture segment boundary (McCalpin, 2009) and displacement could decrease significantly or falls to zero at segment boundaries (Rockwell and Klinger, 2013). But the surface slip distribution of the 1609 earthquake does not show obvious slip impeding or decreasing at this boundary. Because of insufficient data on this rupture section, this geometric complexity cannot be affirmed a segment boundary of the 1609 rupture by the surface slip distribution. The geometry of rupture trace in the Maying River area is much more complex than the HSC (**Figure 14A**). The rupture trace orientation differs by about 30° from the Hongyazi section to the Xiaoquan section, named as Bend 2, and differs by about 70° from the Xiaoquan section to the Maying river section, named as Bend 3, as the dip angles change from 60° to 20°. And there is a step of ~5 km between the eastern segment and the middle segment in this area. This rupture trace complexity and structural discontinuities should indicate a robust segment boundary. It modulated the fault rupture to form a slip troughing on the surface slip distribution (**Figure 14B**), and a slip gap also occurred between Xiaoquan section and the Maying river section. Length of earthquake ruptures is controlled by the geometrical complexity of fault traces (Wesnousky, 2008). Bends and steps in fault trace play a role in controlling the extent of earthquake ruptures (Biasi and Wesnousky, 2017). In previous reports, dip-slip ruptures can cross large steps with maxima of ~5 km (Biasi and Wesnousky, 2016). The orientation of ends of ruptures cannot differ by more than 60° in strike-slip ruptures but it is not clear in dip-slip ruptures, which are observed to have rarely ended at a deflection less than 20°, and maximum angles passed inside ruptures for dip-slip ruptures concentrate below 50° (Biasi and Wesnousky, 2017). The rupture trace and slip distribution of the 1609 earthquake confirmed that The rupture trace and slip distribution of the 1609 earthquake confirmed that large earthquakes can rupture across a large step of ~5 km and a large bend of 70° along a thrust fault.

To further evaluate fault segmentation along the FHF, we synthesized Holocene paleoseismic data from five trench sites in our previous paleo-seismic trenching work (Huang et al., 2018b). The youngest earthquake, constrained to be the AD 1609 earthquake, being evidenced in all the trench sites on three different segments (**Figure 14C**) is consistent to a complete multisegment rupture along the FHF mentioned above. TC3 and TC4, sites on the western segment and middle segment respectively, yielding a time range of 3.4–2.1 ka for the penultimate earthquake, E2, suggest a multisegment rupture. Although the penultimate earthquake in TC2 overlaps the E2, there is a gap between the E2 and the penultimate earthquake in TC1, which is only 100 m apart from TC2. Therefore, the penultimate earthquakes in TC1 and TC2 suggest the third last event, E3, ranged of 4.4–3.5 ka. The E3 evidenced only in TC1 and TC2 could be a single segment rupture, partially ruptured the east segment and was constrained by the Bend 3 and the step in the Maying River area. Both the E2 and E3 were impeded by the large step in this area. TC3, TC2 and TC5 yielding a time range of 7.6–7.0 ka for the fourth last event, E4, suggest another complete multisegment rupture on the FHF, similar with the AD 1609 earthquake. These earthquakes prove that the segment boundaries on the FHF can act as impermanent barriers in single segment rupture or multisegment rupture events, but they cannot impede the rupture propagation of large earthquakes such as the AD 1609 earthquake. The earthquakes alternating between longer multisegment ruptures and shorter single-segment ruptures along the FHF is similar with the Minle-Damaying Fault (thrust fault) in the eastern Qilianshan in China (Lei et al., 2020) and the Wasatch fault zone (normal fault) in United States (McCalpin, 2009; DuRoss et al., 2016).

CONCLUSION

According to our research, the 1609 rupture surface is 98 km long, or 90 km long not including the Shuiguan River section. The surface rupture is mostly vertically offset with an average of 1.0 ± 0.3 m and maximum of 1.8 ± 0.3 m. Lateral horizontal motions occurred locally where the strike departs substantially from mountain front orientation, and a left-lateral offset of 3.0 ± 0.3 m was measured in the easternmost section of the western segment, while some right-lateral offset data were recorded on the Xiaoquan section along the eastern segment with an average value of 1.5 ± 0.3 m. We converted the vertical offsets and lateral offsets (for the area east of Hongshan village and on the Xiaoquan section), to dip slip using the different fault dips on the different segments. The maximum slip is 4.1 + 1.4/−1.2 m based on the offset data collected from points in the area of HCB, and the average slip is 1.8 + 0.6/−0.5, 2.0 + 0.7/−0.6, and 1.8 ± 0.5 m for the western segment, middle segment, and eastern segment, respectively. Constrained by age dating and the historical earthquake catalog, these three segments are considered to have coalesced and ruptured simultaneously during the 1609 earthquake, and we suggest a multisegment rupture for the 1609 earthquake along the FHF.

The moment (Mw) magnitude estimated according to the equations from Hanks and Kanamori (1979), Leonard (2010) and Wells and Coppersmith is approximately Mw 7.2–Mw 7.3 along the FHF from the Hongshuiba River to the Shuiguan River with a length of 90 km. If the Shuiguan River section also broke during the 1609 earthquake, the magnitude could have reached Mw 7.3–Mw 7.4. The rupture trace and slip distribution of the 1609 earthquake confirmed that large earthquakes can rupture across a large step of ~5 km and a large bend of 70° along a thrust fault. The findings of this study should be valuable for future assessments of seismic activity in this region.

DATA AVAILABILITY STATEMENT

The original contributions presented in the study are included in the article/**Supplementary Material**, further inquiries can be directed to the corresponding author.

AUTHOR CONTRIBUTIONS

All authors listed have made a substantial, direct, and intellectual contribution to the work and approved it for publication.

FUNDING

This research was financially supported by National Natural Science Foundation of China (41572195, 42072249) and special funds from China Earthquake Administration for active fault mapping (grant no. 20140823).

SUPPLEMENTARY MATERIAL

The Supplementary Material for this article can be found online at: https://www.frontiersin.org/articles/10.3389/feart.2021.633820/full#supplementary-material.

REFERENCES

Arrowsmith, J. R., Crosby, C. J., Korzhenkov, A. M., Mamyrov, E., Povolostskaya, I., Guralnik, B., et al. (2016). "Surface rupture of the 1911 kebin (Chon–Kemin) earthquake, northern tien Shan, Kyrgyzstan". *In seismicity, fault rupture and earthquake hazards in slowly deforming regions*. Editors A. Landgraf, S. Kuebler, E. Hintersberger, and S. Stein (London, UK: Geological Society, Special Publications), 432, 233–253. doi:10.1144/SP432.10

Biasi, G. P., and Wesnousky, S. G. (2017). Bends and ends of surface ruptures. *Bull. Seismol. Soc. Amer.* 107 (6), 2543–2560. doi:10.1785/0120160292

Biasi, G. P., and Wesnousky, S. G. (2016). Steps and gaps in ground ruptures: empirical bounds on rupture propagation. *Bull. Seismological Soc. America* 106 (3), 1110–1124. doi:10.1785/0120150175

Cao, N., Lei, Z., Yuan, D., and Liu, X. (2010). Textual criticism on the biaoshi, Gansu, earthquake in 180 A D. *Acta Seismol. Sin.* 32 (6), 744–753.

Cao, N. (2010). *Textural research on hongya bao ms71/4 earthquake in 1609 and biaoshi ms71/2 earthquake in 180*, Lanzhou, China: Lanzhou Institute of Seismology.[Master's thesis]CEA 9–43 (in Chinese)

Chen, W. (2003). *Principal features of tectonic deformation and their generation mechanism in the Hexi corridor and its adjacent regions since late Quaternary*. Beijing, China: Institute of Geology, China Earthquake Administration, 36–91.[Dissertation](in Chinese)

Chen, Z. (1994). "Fault activity in Hexi and qilianshan regions," in *In research on earthquake risk in the middle segment of Hexi and qilian Shan region*. Editors T. Shi, Q. Tang, Q. H. Li, and G. Zhao (Beijing: Seismological Press)), 129–147.

Dal Zilio, L., Jolivet, R., and van Dinther, Y. (2020). Segmentation of the main himalayan thrust illuminated by bayesian inference of interseismic coupling. *Geophys. Res. Let.* 47, e2019GL086424. doi:10.1029/2019gl086424

Davis, K., Burbank, D. W., Fisher, D., Wallace, S., and Nobes, D. (2005). Thrust-fault growth and segment linkage in the active Ostler fault zone, New Zealand. *J. Struct. Geology.* 27 (8), 1528–1546. doi:10.1016/j.jsg.2005.04.011

DuRoss, C. B., Personius, S. F., Crone, A. J., Olig, S. S., Hylland, M. D., Lund, W. R., et al. (2016). fault segmentation: new concepts from the Wasatch fault zone, Utah, USA. *J. Geophys. Res. Solid Earth* 121, 1131–1157. doi:10.1002/2015JB012519

Earthquake Disaster Prevention Department (1995). State seismological Bureau. *The catalog of historical strong shocks of China (23 BC to 1911 AD)*. Beijing: Seismological Press, 1–472, 497–499., 508

Earthquake Disaster Prevention Department, China Earthquake Administration (1999). *Recent earthquake catalogue of China (1912~1990, Ms≥4.7)*. Beijing: Chinese Science and Technology Press, 545–548.

Elliott, A. J., Dolan, J. F., and Oglesby, D. D. (2009). Evidence from coseismic slip gradients for dynamic control on rupture propagation and arrest through stepovers. *J. Geophys. Res.* 114, B02312. doi:10.1029/2008JB005969

Gaudemer, Y., Tapponnier, P., Meyer, B., Peltzer, G., Shunmin, G., Zhitai, C., et al. (1995). Partitioning of crustal slip between linked, active faults in the eastern Qilian Shan, and evidence for a major seismic gap, the 'Tianzhu gap', on the western Haiyuan Fault, Gansu (China). *Geophy. J. Int.* 120 (3), 599–645. doi:10.1111/j.1365-246x.1995.tb01842.x

Gu, G. (1983). *Catalogue of Chinese earthquakes*. Beijing: Science Press, 862–894.

Guo, P., Han, Z., Mao, Z., Xie, Z., Dong, S., Gao, F., et al. (2019). Paleoearthquakes and rupture behavior of the Lenglongling fault: implications for seismic hazards of the northeastern margin of the Tibetan Plateau. *J. Geophys. Res. Solid Earth* 124, 1520–1543. doi:10.1029/2018jb016586

Hanks, T. C., and Kanamori, H. (1979). A moment magnitude scale. *J. Geophys. Res.* 84 (B5), 2348–2350. doi:10.1029/jb084ib05p02348

Hetzel, R., Niedermann, S., Tao, M., Kubik, P. W., Ivy-Ochs, S., Gao, B., et al. (2002). Low slip rates and long-term preservation of geomorphic features in Central Asia. *Nature* 417 (6887), 428–432. doi:10.1038/417428a

Hetzel, R., Hampel, A., Gebbeken, P., Xu, Q., and Gold, R. D. (2019). A constant slip rate for the western Qilian Shan frontal thrust during the last 200 ka consistent with GPS-derived and geological shortening rates. *Earth Planet. Sci. Lett.* 509, 100–113. doi:10.1016/j.epsl.2018.12.032

Hetzel, R., Tao, M., Stokes, S., Niedermann, S., Ivy-Ochs, S., Gao, B., et al. (2004). Late Pleistocene/Holocene slip rate of the Zhangye thrust (Qilian Shan, China) and implications for the active growth of the northeastern Tibetan Plateau. *Tectonics* 23. doi:10.1029/2004TC001653

Huang, X., Yang, X., and Yang, H. (2018a). Redetermination of the surface ruptures caused by the Hongyapu, Gansu province, M71/4 earthquake of 1609. *Seismol. Geol.* 40 (1), 276–294. doi:10.3969/j.issn.0253-4967.2018.01.019

Huang, X., Yang, X., and Yang, H. (2018b). Study on paleoearthquakes along the Fodongmiao-Hongyazi fault, Gansu province. *Seismol. Geol.* 40 (4), 753–772. doi:10.3969/j.issn.0253-4967.2018.04.003

Institute of Geology (1993). State seismological bureau, and lanzhou institute of seismology, state seismological bureau. *The qilian mountain-hexi corridor active fault system*. Beijing: Seismological Press, 19–228.

Kumar, S., Wesnousky, S. G., Rockwell, T. K., Briggs, R. W., Thakur, V. C., and Jayangondaperumal, R. (2006). Paleoseismic evidence of great surface rupture earthquakes along the Indian Himalaya. *J. Geophys. Res.* 111, a. doi:10.1029/2004JB003309

Lanzhou Institute of Seismology (1992). *The Changma active fault zone*. Beijing: Seismological Press, 207

Lanzhou Institute of Seismology, State Seismological Bureau (1985). *Strong earthquake catalog in shaanxi, Gansu, ningxia and qinghai pronvinces (1177BC –1982AD)*. Xi'an: Shaanxi Science & Technology Press

Lei, J., Li, Y., Oskin, M. E., Wang, Y., Xiong, J., Xin, W., et al. (2020). Segmented thrust faulting: example from the northeastern margin of the Tibetan Plateau. *J. Geophys. Res. Solid Earth* 125. doi:10.1029/2019jb018634

Leonard, M. (2010). Earthquake fault scaling: self-consistent relating of rupture length, width, average displacement, and moment release. *Bull. Seismological Soc. America* 100 (5A), 1971–1988. doi:10.1785/0120090189

Li, S. (1960). *Chinese earthquake catalogue*. Beijing: Seismological Press

Liu, X., Lei, Z., Yuan, D., and Cao, N. (2011). Textural research on Hongyapu M7 1/4 earthquake in 1609. *Northwest. Seismol. J.* 33 (2), 143–148.

Liu, X., Yuan, D., and He, W. (2014). Preliminary study of paleo-earthquakes on the Fodongmiao-Hongyazi fault in the north margin of qilian mountain. *Technol. Earthquake Disaster Prev.* 9 (3), 411–419.

Liu, X., Yuan, D., Zheng, W., and Cao, N. (2012). Research on late quaternary slip rates of the Fodongmiao-Hongyazi fault at the north margin of qilianshan mountain. *Chin. J. Geol.* 47 (1), 51–61.

Liu, X., Yuan, D., Zheng, W., Shao, Y., Liu, B., and Gao, X. (2019). Holocene slip rate of the frontal thrust in the western Qilian Shan, NE Tibetan Plateau. *Geophys. J. Int.* 219 (2), 853–865. doi:10.1093/gji/ggz325

McCalpin, J. P. (2009). *Paleoseismology*. 2nd edition. Burlington, USA: Academic Press, Elsevier

Meyer, B., Tapponnier, P., Bourjot, L., Métivier, F., Gaudemer, Y., Peltzer, G., et al. (1998). Crustal thickening in Gansu-Qinghai, lithospheric mantle subduction, and oblique, strike-slip controlled growth of the Tibet plateau. *Geophys. J. Int.* 135 (1), 1–47. doi:10.1046/j.1365-246x.1998.00567.x

Molnar, P., and Ghose, S. (2000). Seismic moments of major earthquakes and the rate of shortening across the Tien Shan. *Geophys. Res. Lett.* 27, 2377–2380. doi:10.1029/2000gl011637

Priyanka, R. S., Jayangondaperumal, R., Pandey, A., Mishra, R. L., Singh, I., Bhushan, R., et al. (2017). Primary surface rupture of the 1950 Tibet-Assam great earthquake along the eastern Himalayan front, India. *Sci. Rep.* 7, 5433. doi:10.1038/s41598-017-05644-y

Rockwell, T. K., and Klinger, Y. (2013). Surface rupture and slip distribution of the 1940 imperial valley earthquake, imperial fault, southern California: implications for rupture segmentation and dynamics. *Bull. Seismological Soc. America* 103 (2A), 629–640. doi:10.1785/0120120192

Sapkota, S. N., Bollinger, L., Klinger, Y., Tapponnier, P., Gaudemer, Y., and Tiwari, D. (2013). Primary surface ruptures of the great Himalayan earthquakes in 1934 and 1255. *Nat. Geosci* 6, 71–76. doi:10.1038/ngeo1669

Scholz, C. H. (2002). *The mechanics of earthquakes and faulting*. 2nd edition. Cambridge, UK: Cambridge University Press

Sieh, K. (1996). The repetition of large-earthquake ruptures. *Proc. Natl. Acad. Sci. USA* .93, 3764–3771. doi:10.1073/pnas.93.9.3764

Tapponnier, P., Zhiqin, X., Roger, F., Meyer, B., Arnaud, N., Wittlinger, G., et al. (2001). Oblique stepwise rise and growth of the Tibet Plateau. *Science* 294, 1671–1677. doi:10.1126/science.105978

Tapponnier, P., Meyer, B., Avouac, J. P., Peltzer, G., Gaudemer, Y., Guo Shunmin, S., et al. (1990). Active thrusting and folding in the Qilian Shan, and decoupling between upper crust and mantle in northeastern Tibet. *Earth Planet. Sci. Lett.* 97, 382–403. doi:10.1016/0012-821x(90)90053-z

Thompson, S. C., Weldon, R. J., Rubin, C. M., Abdrakhmatov, K., Molnar, P., and Berger, G. W. (2002). Late quaternary slip rates across the central tien Shan, Kyrgyz republic, central asia. *J. Geophys. Res.* 107 (9), 2203. doi:10.1029/2001jb000596

Wang, K., and Fialko, Y. (2015). Slip model of the 2015 M w 7.8 Gorkha (Nepal) earthquake from inversions of ALOS-2 and GPS data. *Geophys. Res. Lett.* 42, 7452–7458. doi:10.1002/2015GL065201

Wells, D. L., and Coppersmith, K. J. (1994). New empirical relationships among magnitude, rupture length, rupture width, rupture area, and surface displacement. *Bull. Seismol. Soc. Amer.* 84 (4), 974–1002.

Wesnousky, S. G. (2008). Displacement and geometrical characteristics of earthquake surface ruptures: issues and implications for seismic-hazard analysis and the process of earthquake rupture. *Bull. Seismological Soc. America* 98 (4), 1609–1632. doi:10.1785/0120070111

Xu, X., Yeats, R. S., and Yu, G. (2010). Five short historical earthquake surface ruptures near the silk road, gansu province, China. *Bull. Seismological Soc. America* 100 (2), 541–561. doi:10.1785/0120080282

Yang, H., Yang, X., Huang, W., Li, A., Hu, Z., Huang, X., et al. (2020). 10Be and OSL dating of Pleistocene fluvial terraces along the Hongshuiba River: constraints on tectonic and climatic drivers for fluvial downcutting across the NE Tibetan Plateau margin, China. *Geomorphology* 348, 106884. doi:10.1016/j.geomorph.2019.106884

Yang, H., Yang, X., and Huang, X. (2017). A preliminary study about slip rate of middle segment of the Northern qilian thrust fault zone since late quaternary. *Seismol. Geol.* 39 (2), 20–42. doi:10.3969/j.issn.0253-4967

Yang, H., Yang, X., Huang, X., Huang, W., and Luo, J. (2016). Data comparative analysis between SFM data and DGPS data: a case study from fault scarp in the east bank of Hongshuiba River, northern margin of the qilian Shan. *Seismol. Geol.* 38 (4), 1030–1046.

Yang, H., Yang, X., Huang, X., Li, A., Huang, W., and Zhang, L. (2018a). New constraints on slip rates of the Fodongmiao-Hongyazi fault in the Northern Qilian Shan, NE Tibet, from the 10Be exposure dating of offset terraces. *J. Asian Earth Sci.* 151, 131–147. doi:10.1016/j.jseaes.2017.10.034

Yang, H., Yang, X., Zhang, H., Huang, X., Huang, W., and Zhang, N. (2018b). Active fold deformation and crustal shortening rates of the qilian Shan foreland thrust belt, NE Tibet, since the late Pleistocene. *Tectonophysics* 742-743, 84–100. doi:10.1016/j.tecto.2018.05.019

Yang, S., Cheng, X., Xiao, A., Chen, J., Fan, M., and Tain, D. (2007). *The structural characteristics of Northern Qilian Shan Mountain thrust belt and its control on the oil and gas accumulation*. Beijing, China: Science Press

Yeats, R. S., Sieh, K., and Allen, C. R. (1996). *The Geology of earthquakes*. New York: Oxford University Press

Yuan, D. Y., Ge, W. P., Chen, Z. W., Li, C. Y., Wang, Z. C., Zhang, H. P., et al. (2013). The growth of northeastern Tibet and its relevance to large-scale continental geodynamics: a review of recent studies. *Tectonics* 32 (5), 1358–1370. doi:10.1002/tect.20081

Yue, L.-F., Suppe, J., Hung, J.-H., and Hung, J.-H. (2005). Structural geology of a classic thrust belt earthquake: the 1999 Chi-Chi earthquake Taiwan (Mw=7.6). *J. Struct. Geology.* 27 (11), 2058–2083. doi:10.1016/j.jsg.2005.05.020

Zhang, P.-Z., Shen, Z., Wang, M., Gan, W., Bürgmann, R., Molnar, P., et al. (2004). Continuous deformation of the Tibetan Plateau from global positioning system data. *Geol.* 32 (9), 809–812. doi:10.1130/g20554.1

Zhang, P., Deng, Q., Xu, X., Peng, S., and Yang, X. (1994). Blind thrust, folding earthquake, and the 1906 manas earthquake, xinjiang. *Seismol. Geol.* 16 (3), 193–204.

Zheng, W.-j., Zhang, P.-z., He, W.-g., Yuan, D.-y., Shao, Y.-x., Zheng, D.-w., et al. (2013). Transformation of displacement between strike-slip and crustal shortening in the northern margin of the Tibetan Plateau: evidence from decadal GPS measurements and late quaternary slip rates on faults. *Tectonophysics* 584, 267–280. doi:10.1016/j.tecto.2012.01.006

Zheng, W. (2009a). *Geometric pattern and active tectonics of the Hexi Corridor and its adjacent regions*. Beijing, China. Earthquake Administration: Institute of Geology

Zheng, W., Zhang, P., Yuan, D., Ge, W., and Liu, J. (2009b). Discovery of surface rupture zone on the south of helishan in gaotai, gansu province. *Seismol. Geol.* 31 (2), 247–255. doi:10.3969/j.issn.0253-4967.2009.02.005

Zuza, A. V., Cheng, X., and Yin, A. (2016). Testing models of tibetan plateau formation with cenozoic shortening estimates across the qilian shan-nan shan thrust belt. *Geosphere* 12 (2), 501–532. doi:10.1130/ges01254.1

Conflict of Interest: The authors declare that the research was conducted in the absence of any commercial or financial relationships that could be construed as a potential conflict of interest.